Characterization of Putative Mammalian Adenylyl Cyclase Inhibitors Using the Fission Yeast *Schizosaccharomyces pombe*

Daniel Peter Pacella

An Undergraduate thesis

presented to the Faculty of

the Department of Biology

in partial fulfillment

of the requirements for the degree of

Bachelor of Science in Biology

and in fulfillment of

Scholar of the College Candidacy

Boston College
Chestnut Hill, MA
Morrissey College of Arts and Sciences

April 2022

Characterization of Putative Mammalian Adenylyl Cyclase Inhibitors Using the Fission Yeast *Schizosaccharomyces pombe*

By: Daniel Peter Pacella

Advisor: Charles Stuart Hoffman, Ph.D.

ABSTRACT

In both mammals and fission yeast, control of cAMP levels is maintained by adenylyl cyclases (ACs), which synthesize cyclic nucleotide, and by cyclic nucleotide phosphodiesterases (PDEs), which are responsible for its degradation. AC activity is regulated by G proteins, which respond to signals from G protein-coupled receptors (GPCRs) that detect extracellular signaling factors such as hormones. cAMP is a second messenger that has several effectors, with protein kinase A (PKA) being a primary target of activation that phosphorylates several downstream targets and results in modulation of pathways such as cell growth and gluconeogenesis. Aberrant cAMP regulation has been linked to several human disease states, such as McCune-Albright Syndrome, which is the result of elevated cAMP levels. Whereas the targeting of PDEs with drugs and selective inhibitors has been very successful, the AC-inhibiting compounds identified to date are unfavorable for clinical use. Inhibitors may not necessarily bind to and inhibit a given AC directly but instead act on a regulatory pathway such as calmodulin signaling. Theoretically, they also may bind to the G protein, interfere with the AC-G protein stimulatory complex, or regulate a factor of *AC* transcription. Since more than one AC species is expressed in many human cell types, it is difficult to selectively reduce cAMP levels. Therefore, for an AC inhibitor to be favored as a candidate for drug development, it is likely that the compound should directly bind to and inhibit the AC. This thesis

describes my studies on a scaffold of 41 structurally related BCAC compounds, called the BCAC51 scaffold, that was identified in a high-throughput screen (HTS) with *Schizosaccharomyces pombe* strains transformed with GNAS and either mammalian AC4 or AC7. I carried out a series of experiments to examine whether the compounds bind to and inhibit mammalian ACs directly. The most active compounds were further characterized for potency and specificity against a panel of ACs. Several compounds significantly reduced cAMP production, but it could not be determined if the compounds directly or indirectly altered AC activity. I also cloned and constructed strains expressing the human wild-type AC5 gene and the AC5 R418W mutant, which has shown an increased sensitivity to GNAS. cAMP assays on these strains using various BCAC compounds showed that while most compounds had similar effects on both forms of AC5, BCAC62 was significantly more effective on the wild-type enzyme than on the mutant AC5, although the reason for this is unclear. To test whether the compounds could reduce AC activity in the absence of GNAS (basal activity), a flow cytometry study was carried out using a PKA-repressed GFP reporter. Results suggested that BCAC compounds do reduce basal-AC activity and therefore do not act by binding to and inhibiting GNAS, by interfering with the AC-GNAS stimulatory complex, nor by stimulating PDE. Finally, I developed a molecular genetic screen for mutant alleles of an AC gene that confer compound-resistance. One cycle of the screen is near completion, and the screen provides a foundation for future examination of compound-resistant AC candidates. The results presented in this thesis serve as a basis for further research into members of the BCAC51 compound series being putative direct inhibitors of mammalian ACs.

TABLE OF CONTENTS

LIST OF TABLES

LIST OF FIGURES

ACKNOWLEDGMENTS

First and most importantly, I extend my most heartfelt gratitude to my advisor and mentor, Dr. Charles “Charlie” Hoffman. It is rare to find somebody in an academic context who teaches you the way that Charlie does. I have truly never encountered anyone during my university experience who treated me as an equal so much as Charlie. Even amidst the intellectually rigorous, productive, and stimulating environment of his laboratory, Charlie took every moment he could to get to know me and my intellectual habits so that he could adjust his style of mentorship accordingly. Working in his lab has been the most intense and rewarding learning experience of my academic career, both scholastically and personally. I was given the responsibility to take ownership of my project whilst being encouraged to always ask deeper questions about my experiments and the concepts behind them. All the while, Charlie’s willingness to get to know myself and all his other students in an empathetic way is remarkable, especially given the pedagogical challenges that came with the COVID-19 pandemic. I will always owe my potential success and many of the lessons I learned to Charlie, and I will forever remember the time spent under his wing.

I also sincerely thank my family. Without my mother and father and the personal, emotional, and financial sacrifices that they have made for me during my entire life, I would not be the person that I am today. I am certain that I would not be able to complete this thesis or to graduate without the support that they constantly provide for me. Thank you, Mom and Dad, for coaching me through several mental hardships and for showing me what it means to be truly loved.

To my professors, I came into college as an overwhelmed and anxious student and left as a confident citizen-scientist; all of that is owed to you. While the amount of faculty whom I admire is innumerable, there are certain people to whom I owe my utmost gratitude. I am most grateful

for Professor Doug Warner's consistent care and mentorship throughout my four years. From Molecules and Cells to grading this thesis, you truly have been a "full circle" presence and will always make such a positive impact on many students' careers. I am equally indebted to Professor Holly Deak for being a source of empathy, support, and inspiration during the several opportunities she has created to enable my success. Thank you to Professor Danielle Taghian for always being so insightful, caring, and self-sacrificing for both myself and everyone you meet. To Professor Ismael Fofana, I greatly cherish your joyful presence as much as I do the sincere efforts you give toward each one of your students and mentees. To Dr. Jeremy Eberhard, thank you for your consistently helpful knowledge and encouragement; our lab would not be the same without you. The data collection done to prepare this thesis would have been impossible without Dr. Patrick Autissier, Manager of the Boston College Flow Cytometry Facility and without Mr. Marek Domin, Director of Mass Spectrometry. I am also very appreciative of Professor Anthony Annunziato for being so generous in lending me much of his lab space. I am very thankful for Professor Jeff DaCosta as well, as he was very helpful in performing statistical analysis throughout much of this project.

To my friends and colleagues, words cannot express how much I appreciate your being in my life. To Joe and Marissa, thank you for teaching me what it means to be a passionate scientist and also a kind, loyal friend. To my roommate, Henry, I will never forget your true companionship and thoughtfulness. To Oliver and John, your hard work and commitment to your studies has inspired me. To my lab-mates, Judy, Erik, Esther, and Maira, your encouragement means the world to me; I cannot wait to see your successes someday as scientists and healthcare professionals.

LIST OF ABBREVIATIONS

cAMP	cyclic adenosine monophosphate
ATP	adenosine triphosphate
AC	adenylyl cyclase
PDE	cyclic nucleotide phosphodiesterase
GTP	guanosine triphosphate
GDP	guanosine diphosphate
G protein	heterotrimeric guanine nucleotide-binding protein
GPCR	G protein-coupled receptor
PKA	protein kinase A
HTS	high-throughput screen
BCAC	Boston College Adenylyl Cyclase putative inhibitor compound
GNAS	guanine nucleotide alpha-stimulating protein
GFP	green fluorescent protein
Fbp1	fructose-1,6-biphosphatase
Ura4	OMP decarboxylase
MAPK	mitogen-activated protein kinase
YES	yeast extract medium
EMM	Edinburgh Minimal Medium
FACS	fluorescent-activated cell sorting
Q3/Q4	Quadrant 3/Quadrant 4 border in flow cytometry
MFI	median fluorescent intensity
Git	glucose-insensitive transcription

1 INTRODUCTION

1.1 The Second Messenger cAMP

Cyclic adenosine monophosphate (cAMP) is an important second messenger in a wide range of organisms that is intracellularly synthesized in response to extracellular signals (Robison *et al.* 1968). cAMP levels regulate a wide array of biological processes, enabled by cAMP's binding to a variety of downstream effectors. These include protein kinase A (PKA), a tetrameric cAMP-dependent serine/threonine kinase, and cyclic nucleotide-gated channels (Biel *et al.* 2009, Hoffman 2005a). cAMP binds to the regulatory subunits of PKA to trigger a cascade of downstream phosphorylation that leads to the activation or inactivation of several proteins, including transcription factors. These proteins mediate such cellular processes as passage through the cell cycle and gluconeogenesis in mammals and sexual development and metabolism in *Schizosaccharomyces pombe*.

cAMP levels are controlled by two families of proteins: adenylyl cyclases (ACs) catalyze the synthesis of 3-5'cAMP (and inorganic pyrophosphate) from ATP, and cyclic nucleotide phosphodiesterases (PDEs) hydrolyze cAMP to form 5'AMP (Kamenetsky *et al.* 2006, Getz *et al.* 2019).

1.2 Mammalian Adenylyl Cyclases (ACs) and G Protein-Mediated PKA Signaling

There are ten class III mammalian AC enzymes, one of which is soluble (sAC/AC10), while the other nine are integral transmembrane proteins (tmACs/AC1-AC9). The tmACs comprise 4 families, grouped based upon differences in regulatory mechanisms by heterotrimeric guanine

nucleotide-binding (G) proteins and other signal transductors, their membrane environment, and their sensitivity to the plant-derived diterpene forskolin (Dessauer *et al.* 2017). The ACs described in this thesis are derived from the following organisms: *Homo sapiens* (AC1, 2, 5, 7, 9), *Rattus norvegicus* (AC3, 4, 8, and sAC), and *Canis lupis* (AC6) (Getz *et al.* 2019). The mammalian ACs are integrators for a variety of stimulatory and inhibitory signals. Agonists and antagonists, including intermediate metabolite-ligands that trigger nutrient uptake (Husted *et al.* 2017) and growth hormones (Pavlos *et al.* 2017), bind to 7-transmembrane-domain surface G protein-coupled receptors (GPCRs), which are upstream of the G proteins G_s and G_i (Rodbell 1995, Chang *et al*. 2016). G proteins are GTPases that regulate the action of ACs, as determined by the binding state between their various subunits and AC (Simonds 1999). G_s stimulates all of the transmembrane ACs: the interaction of the $G_s\alpha$ subunit with GTP maintains the AC's active state until its reassociation with both the $G_s\beta\gamma$ dimeric subunit and GDP following stimulation from a GPCR and a conformational change (Lambright *et al*. 1996). The only $G_s\alpha$ protein in mammals is GNAS (Chang *et al*. 2016). Mutations in GNAS leading to the protein's activation are associated with elevated cAMP levels and are implicated in several disease states, including McCune-Albright Syndrome (MAS, OMIM #174800), an osteoblastic fibrous dysplasia, as well as café-au-lait disorder of the skin and neoplastic transformation of endocrine cells (Chang *et al*. 2016, Weinstein *et al*. 2006, Levine 1999). Inhibition of some ACs by $G_i\alpha$ (AC3, 5, 6) occurs through a direct binding of the subunit and AC. Activation of the $G\beta\gamma$ heterodimeric subunit of G_i also occurs following stimulation of the G_i-GPCR complex, which activates effector complexes such as Src and ERK1/2 (Simonds 1999, Chang *et al*. 2016).

G protein-mediated signaling, affecting AC catalysis of cAMP production and thus PKA activation, is well-conserved between mammals and fission yeast. Therefore, *S. pombe* is a suitable model organism for studying the mammalian ACs.

1.3 Phosphodiesterases (PDEs)

All mammalian PDEs are classified as Class I enzymes, as they catalyze the hydrolysis of the 3' cyclic phosphate bond of cAMP in a highly selective manner. Class I PDEs are grouped into 11 functional, pharmacological families based on variation in their isomorphic tertiary structures and their modes of regulation. The 11 PDEs are encoded by 21 different genes, but these genes produce at least 100 isoforms (Bender and Beavo 2006).

1.4 Feasibility and Successes of PDEs as Drug Targets

PDEs are favorable drug targets for a variety of reasons. Multiple types of PDEs are found in nearly every tissue of the mammalian organism and are responsible for several different macro-scale functions and associated disease states, such as chronic obstructive pulmonary disease (COPD), when functional (Burgin *et al.* 2010). The pharmacokinetic principle that inhibition of the "agent of degradation" of a second messenger such as cAMP is more attractive due to its relatively higher rate of action than its synthesizing agent has made PDEs a druggable target since their discovery. Furthermore, the diversity of unique structures of the catalytic cleft among PDE families makes PDEs easier to selectively inhibit, as does the fact that cAMP levels in mammals often do not reach higher than 10μM and can thus be competitively outcompeted (Bendo and Beavo 2006). A variety of inhibitors to PDEs have been identified and have led to the development of clinically successful drugs, including several potent antineoplastics and

antidepressants as well as agents used to treat erectile dysfunction and COPD (Yamamoto *et al.* 1983, Burgin *et al.* 2010). Drug development has occurred through a process of structure-based modification and biological assay. PDE inhibitors have also been important in helping to understand the biological role of the enzyme itself: inhibitors to specific families have revealed the pathways in which they are a part (Maurice *et al.* 2014).

1.5 Drug Development Efforts with ACs have been Relatively Lacking

AC inhibitors have been developed, the majority of which target the enzyme's catalytic cleft. Inhibitor compounds that employ three different mechanisms of action have been isolated: noncompetitive, competitive, and "activity-dependent" (Seifert *et al*. 2012). However, there are limitations to these inhibitors. The potency of inhibitors on any given AC is difficult due to a concept of pharmacokinetics: more than one AC species is expressed in many cell types, which would result in a high dosage of inhibitor needed to achieve an effect on any one target AC (Dessauer *et al.* 2017). The amount of inhibitor required would result in toxicity and severe side effects to humans (Dessauer *et al.* 2017, Steegborn *et al.* 2014, Levin and Buck 2015). Some have suggested that a localized application of inhibitors could be a strategy for drug development, such as an application to the eye (Roth and Amory 2016), although one can envision a very limited and financially unfavorable drug application in this case. Therefore, development of AC inhibitors into drugs has been mainly silent, and this is a need that remains unmet.

1.6 The *fbp1:ura4* and *fbp1:GFP* Reporters: Tools to Measure PKA Activity

The construction of fusion proteins consisting of reporter genes fused to the *S. pombe fbp1* promoter has been useful in the determination of some phenotypes related to PKA activity, as these reporter genes are repressed by PKA activity (Figure 1). The *fbp1* gene encodes the gluconeogenic enzyme fructose-1,6-biphosphatase and is subject to transcriptional repression in the presence of extracellular glucose (Vassarotti and Friesen 1985, Hoffman and Winston 1989). The *ura4* gene, which encodes the enzyme OMP decarboxylase that is used to catalyze the synthesis of uracil, has been employed to construct the *fbp1:ura4* fusion. The reporter's integration allows for selection in growth medium lacking uracil. In wild-type strains grown in a glucose-rich environment, *fbp1* is transcriptionally repressed by PKA, and thus cells are Ura^-; conversely, glucose-starved conditions yield cells that are Ura^+. The reporter also enables "counterselection" in the presence of the pyrimidine analog 5-fluoroorotic acid (5FOA), since expression of *ura4* prevents growth in this condition. Therefore, in wild-type strains, a glucose-rich environment will yield a high-PKA phenotype and 5FOA resistance ($5FOA^R$), and a glucose-starved environment will yield 5FOA-sensitive cells ($5FOA^S$).

Figure 1. The *fbp1:ura4* reporter can be used to assess a variety of PKA-associated phenotypes in different environmental glucose states. Cells are uracil-deficient (Ura^-) and resistant to 5FOA ($5FOA^R$) in the presence of glucose, and they produce uracil (Ura^+) and are sensitive to 5FOA ($5FOA^S$) when starved of glucose.

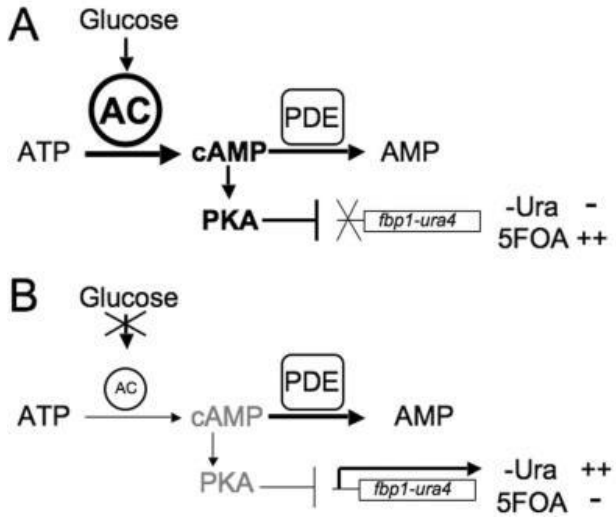

Adapted from:

Ivey FD, Wang L, Demirbas D, Allain C, Hoffman CS. Development of a fission yeast-based high-throughput screen to identify chemical regulators of cAMP phosphodiesterases. J Biomol Screen. 2008 Jan;13(1):62-71.

The *Aquorea victoria* green fluorescent protein (GFP) gene encodes a protein very useful in biochemical assays, such as fluorescence microscopy or flow cytometry. Construction and expression of the *fbp1:GFP* reporter in *S. pombe* has also allowed for a phenotypic assay, as fluorescence is inversely related to PKA activity.

Other phenotypes that are not measurable with the *fbp1:ura4* or *fbp1:GFP* fusions, but are still under control of PKA activity, are included in Table 1. These are observed as a consequence of

PKA's transcriptional regulation of several genes involved in a variety of cell processes, such as response to external stress, growth, sexual development, and metabolism (de Madeiros *et al*. 2013). For instance, PKA inhibits transcription of *mei2*, which directs the replication of DNA pre-meiotically and the absence of which confers arrest of the cell cycle before S-phase (Yamamoto 1996). High PKA activity, therefore, corresponds to partial sterility (Devoti *et al.* 1991).

Table 1. Phenotypes associated with Relative PKA Activity Levels in *S. pombe*

Process or Reporter	**High-PKA Phenotype**	**Low-PKA Phenotype**
Doubling time	~3 hours	4-6 hours
Cell length at septation	15-17 microns	10-12 microns
Sexual development	Partial sterility	Sexually competent
Stationary phase entry	Defective: rapid cell death	Successful entry
Salt stress	KCl-resistance	KCl-sensitivity
fbp1:lacZ	Low β-gal activity	High β-gal activity
fbp1:GFP	Low fluorescence	High fluorescence
fbp1:ura4	$5FOA^R$; Ura^-	$5FOA^S$; Ura^+

1.7 Molecular Genetics Reveal the Genes Necessary for cAMP Signaling in Fission Yeast

As part of a classical molecular genetics investigation into glucose signaling using the fission yeast *S. pombe*, the genes involved in the pathway that leads to cAMP production were identified. Mutations that resulted in the constitutive expression of the *fbp1:ura4* translational fusion in the presence of glucose led to the identification of 10 *git* (glucose-insensitive transcription) genes, mutations in which led to a significant derepression of transcription of *fbp1*

in the presence of exogenous 8% glucose and cAMP supplemented to the growth medium (both are transcriptional repressors) (Hoffman and Winston 1990, 1991).

The *git2* gene encodes adenylyl cyclase, as suggested by the derepression of transcription of *fbp1* in a *git2* null mutant and the restoration of repression upon cell re-exposure to exogenous cAMP. Repression of *fbp1* is caused by cAMP's activation of PKA, which phosphorylates downstream signaling proteins, upon activation of adenylyl cyclase after exposure to glucose (Hoffman and Winston 1991). Six other *git* genes were later found to activate adenylyl cyclase, and another gene encodes the catalytic subunit of PKA. Several of *git* were then found to synthesize subunits of a heterotrimeric G protein involved in cAMP signaling: *git8*, otherwise known as *gpa2*, encodes the Gα subunit, *git5* encodes the Gβ subunit, and *git11* encodes the Gɣ subunit. As with other G proteins, regulation of effectors occurs via the Gα and Gβɣ subunits. When Gα is bound to GDP, the protein is inactive; stimulation from ligand-binding to a GPCR exchanges Gα's binding from GDP to GTP as well as a conformational change that alters Gα's affinity for Gβɣ. *git3* was later found to encode a GPCR, and it is speculated that the Gβɣ dimer facilitates the association of the Git3 receptor with the Gpa2 Gα subunit for Git3 to stimulate the G protein. The Gpa2 Gα subunit directly binds to and activates the AC. The G protein-mediated PKA signaling pathway in *S. pombe* is shown (Hoffman 2005a; Hoffman 2005b) (Figure 2).

Figure 2. G protein-mediated signaling in the fission yeast *S. pombe* responds to detection of glucose through cAMP synthesis, which in turn activates PKA. A cascade of phosphorylation subsequently affects the transcription of several genes, such as the repression of *fbp1*. A number of *git* genes moderate this signal transduction pathway.

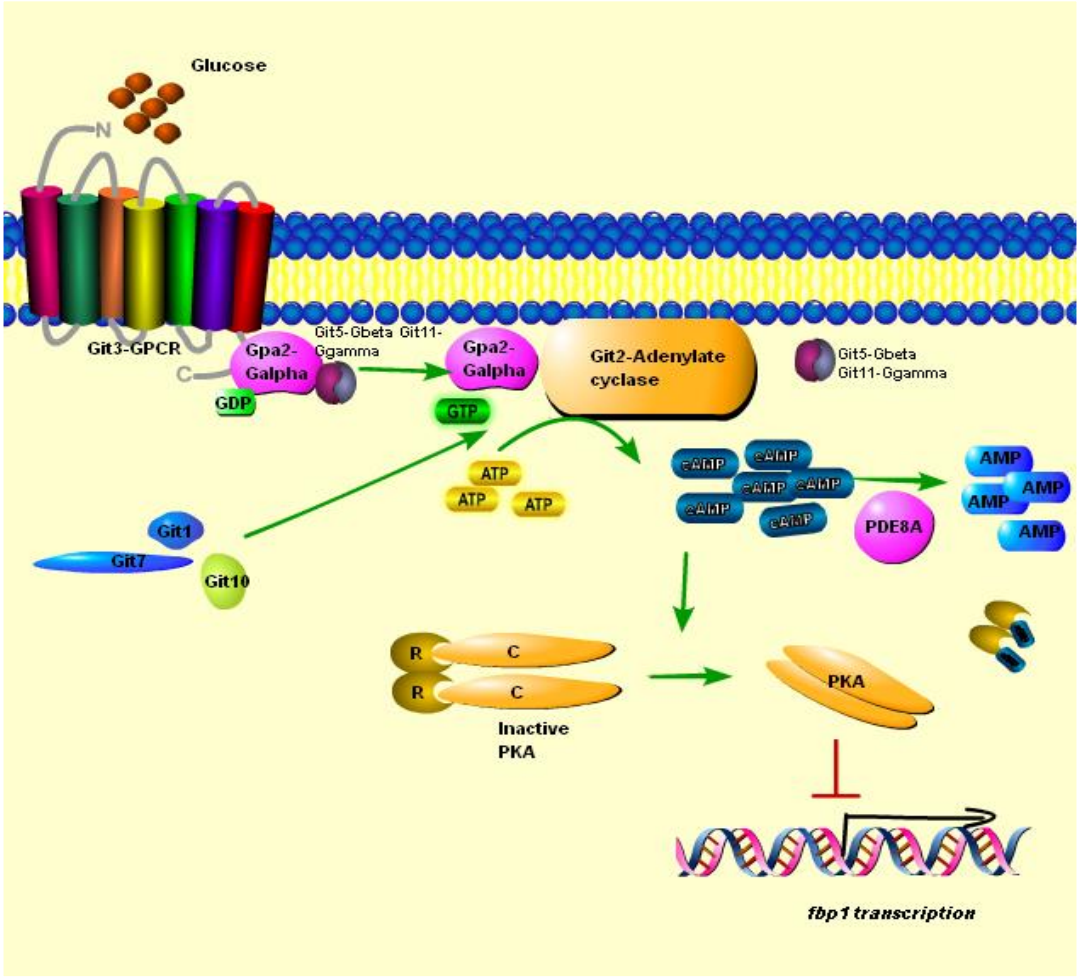

1.8 *fbp1* Transcription also Responds to Cell Stress Signaling

Transcription of *fbp1* is also monitored by extracellular stress. Stress conditions, such as glucose-starvation or severe physical or temperature disturbance, trigger a mitogen-activated protein kinase (MAPK) signaling pathway initiated by the MAPKK kinases (MAPKKK) Wis4 and

Win1. These phosphorylate the Wis1 MAPK kinase (MAPKK), which itself activates the MAPK Spc1 (Stiefel *et al.* 2004). Spc1 phosphorylates the downstream Atf1-Pcr1 heterodimer that transcriptionally activates *fbp1* (Neely and Hoffman 2000) (Figure 3). Thus, in wild-type cells, *fbp1* regulation remains under dual control: transcription is derepressed in response to stress and repressed in response to glucose detection.

Figure 3. In *S. pombe*, the response to stress consists of a MAPK signaling cascade. In the final step of the pathway, the MAPK Spc1 (Sty1) phosphorylates Atf1 of the Atf1-Pcr1 heterodimer to activate transcription of *fbp1*. Alternatively, PKA, which is activated in the presence of extracellular glucose, represses *fbp1* transcription. Spc1 is itself phosphorylated by the MAPKK Wis1, which is activated by the MAPKKKs Wis4 and Win1.

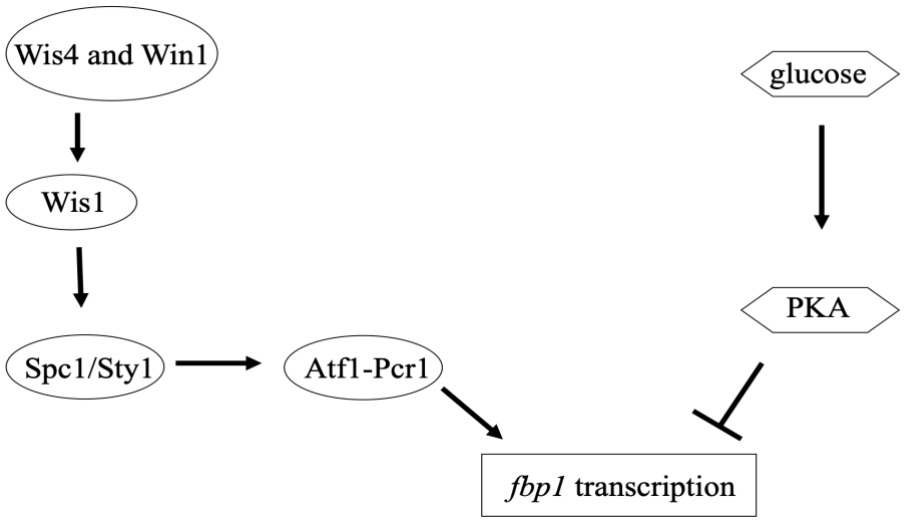

1.9 Yeast-Based Screens with the *fbp1:ura4* reporter

Research hypotheses in the field of chemical genetics often call for the investigation of a small-molecule probe that targets a protein of interest. The use of high-throughput screens (HTSs) to

identify compounds of interest has become a successful and widely used method for identifying novel small-molecule probes for biological targets since the 1990s. Many efforts to develop inhibitors to PDEs and ACs have employed HTSs.

S. pombe cells that carry the *fbp1:ura4* reporter allow for successful yeast-based HTSs to be conducted, in order to determine potentially potent inhibitors to PDEs. The screens have allowed for the detection of potent PDE inhibitors, including those to PDE4, PDE5, PDE7, PDE8, and PDE11. The screens were 5FOA growth readout assays that functioned as follows. As cells with high PKA activity grow in the presence of 5FOA, and a PDE inhibitor would increase PKA activity, hit compounds could be detected based on their ability to revert a 5FOA-sensitive ($5FOA^{s}$) strain carrying the *fbp1:ura4* reporter to grow in the presence of 5FOA ($5FOA^{R}$). Hit compounds also needed to be cell permeable and stable for the 48-hour growth period employed during this screen (Hoffman 2022).

A HTS was used to detect hit compounds that inhibited mammalian ACs or the stimulatory $G_s\alpha$ subunit of GNAS. The screen used the PKA-repressed *fbp1:GFP* reporter, with AC activity being shown using fluorescence assays and mass spectrometry (measuring cAMP levels), and was tested on strains expressing mammalian ACs. The ability of a compound to effectively lower intracellular cAMP levels was expected to occur through one of four possible mechanisms: inhibition of adenylyl cyclase directly, inhibition of GNAS, inhibition or obstruction of the GNAS-AC stimulatory complex during interaction, or stimulation of a PDE. In the HTS, diphenyleneiodonium chloride (DPI) was identified as a highly potent inhibitor of AC9. DPI lowered cAMP production in a strain expressing the basal-AC9 gene, and DPI had a weak

inhibitory effect on AC6. This suggests that DPI does not bind to and inhibit GNAS. DPI is still effective on strains that express several PDEs, including PDE4 in the presence of the PDE4 inhibitor Rolipram, which suggests that DPI does not stimulate a PDE to lower cAMP levels in cells (Getz *et al.* 2019).

1.10 Identification of Putative Adenylyl Cyclase Inhibitors

A scaffold of 41 putative inhibitor compounds (Boston College Adenylyl Cyclase 51, BCAC51, scaffold) was previously identified in a HTS conducted by the Hoffman lab (unpublished data). These compounds are all highly similar in their chemical structure. Preliminary experiments have suggested that these compounds have different potencies to various mammalian ACs. Val Watts' lab identified the same scaffold in a cell-based screen involving membrane extracts of AC1 under stimulation of the A23187 calcium ionophore (Kaur *et al.* 2019). However, samples failed to show activity in an enzyme assay *in vitro*. They concluded that the compounds do not directly inhibit the AC and instead interfere with the calmodulin signaling pathway that is required for AC1 stimulation (Val Watts, pers. comm.). However, the Hoffman lab screen involved fission yeast strains expressing either AC4 or AC7 together with a mutationally-activated GNAS ($GNAS^{R201C}$) and would thus not be influenced by calcium signaling. Therefore, the possibility that the BCAC51 scaffold is active on adenylyl cyclase is of interest.

1.11 The GNAS-Sensitive R418W Mutation in Human AC5

The R418W polymorphism in human AC5 has been shown to confer increased sensitivity to GNAS and is implicated in several diseases, such as familial dyskinesia (Dessauer *et al.* 2017). This mutation is located in a linker region of the adenylyl cyclase, between the M1

transmembrane domain and the catalytic domain C1 (containing the ATP-hydrolyzing active site), as pointed out in the AC5 schematic (Figure 4). As this mutation affected GNAS-mediated activation, we wanted to investigate whether this AC5 mutant would respond differently than wild-type loci to putative inhibitor compounds.

Figure 4. The R418W gain-of-function mutation in human AC5 has shown an increased sensitivity to GNAS. The mutation is located in a linker region before the first catalytic domain (C1a) and the M1 transmembrane domain.

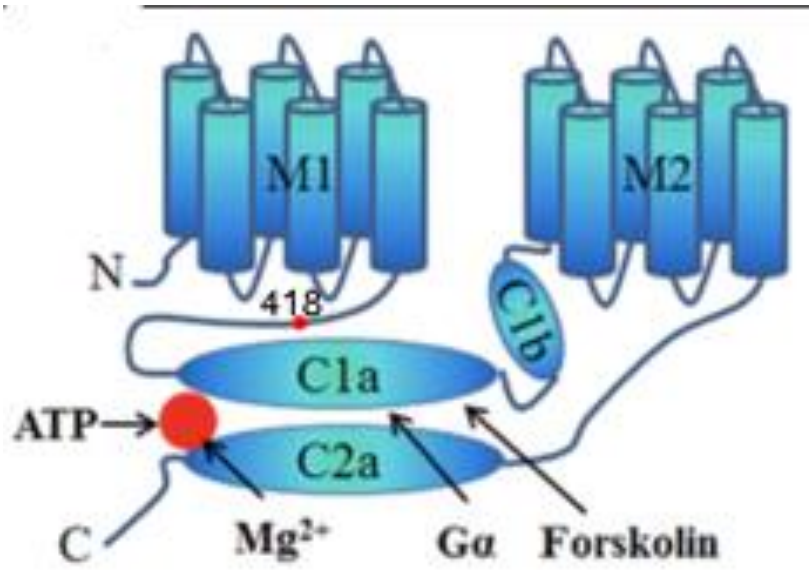

1.12 Research Objective

This project was designed to address the question of whether compounds of the BCAC51 scaffold bind to and inhibit mammalian ACs directly or whether they indirectly reduce cAMP production. Indirect mechanisms of compound action include modulation of an object of a pathway that regulates AC activity, inhibition of GNAS, interference with the GNAS-AC stimulatory complex, or stimulation of PDE activity. Since all 10 ACs are expressed in many

human cell types, it is difficult to selectively reduce cAMP levels (Dessauer *et al.* 2017). Therefore, for an AC inhibitor to be favored as a candidate for drug development, it is likely that the compound's direct binding to the AC will be a very supportive characteristic.

The goals of this project were four-fold. The first goal was to identify the most active of the 41 compounds of the BCAC51 scaffold series and characterize their activity. Several compounds significantly reduced cAMP production, but more repetition of experiments is needed to determine if the compounds preferentially bind to and inhibit the ACs (act directly). The second goal was to characterize the wild-type and R418W-mutant AC5 alleles by their sensitivity to BCAC compounds. The alleles were shown to respond with similar significance to all compounds except for BCAC62. The third goal was to examine whether compounds could affect AC activity in the absence of GNAS (basal activity). The results suggest that BCAC compounds do not act by binding to and inhibiting GNAS directly, by interfering with the AC-GNAS stimulatory complex, nor by stimulating PDE activity. The fourth goal was to design a molecular genetic screen for mutations in an AC gene that confer BCAC compound-resistance. The potential screen was developed that provides a foundation for further isolation and examination of compound-resistant candidates. This research should be complemented with experimental repetition in an effort to characterize the mechanism of action of members of the BCAC51 series conclusively.

2 MATERIALS AND METHODS

2.1 MATERIALS

2.1.1 Growth Media

The standard medium used to grow and maintain *Schizosaccharomyces pombe* was a yeast extract medium with nutritional supplements (YES), prepared as described by Gutz (Gutz *et al.* 1974). Edinburgh minimal medium (EMM) was used for liquid cultures and was supplemented with leucine, lysine, histidine, adenine, and uracil (75 mg/L for all except L-leucine, which was at 150 mg/L) required for strain growth. To grow *Escherichia coli*, LB (1% tryptone, 0.5% yeast extract, 1% NaCl) was used.

2.1.2 Yeast

The *S. pombe* strains used throughout all experiments are listed in Table 2. Most strains carried the *fbp1:GFP* translational fusion, used as a reporter. Yeast was grown at 30℃.

Table 2. Strain List

Strain	h	his7	Other Markers	*git*	*nft*
CHP731	+	+	his3-D1	+	+
CHP1466	+	his7-366	pap1D::ura4- cgs2::PDE4D2	git2-2::his7+(7)	+
CHP1744		+	pap1::ura4- cgs2::ratPDE4A5	git11::kan	+
CHP1760		+	pap1::ura4- cgs2::ratPDE4A5	git3::kan	+
CHP1817	-	+	pap1D::ura4- cgs2::PDE4D2 [pLEV3-AC7] ars1[pNMT1-GNAS1R201C LEU2+]	git2-2::his7+(7)	
CHP1826	-	+	pap1D::ura4- cgs2::PDE4D2 [pLEV3-AC4] ars1[pNMT1-GNAS1R201C LEU2+]	git2-2::his7+(7)	
CHP1829	+	+	pap1D::ura4- cgs2::PDE4D2 [pLEV3-AC7]	git2-2::his7+(7)	
CHP1831	-	+	lys2-97 pap1D::ura4- cgs2::PDE4D2 ars1[pNMT1-GNAS1R201C LEU2+]	git2-2::his7+(7)	
CHP1892	+	+	pap1D::ura4- cgs2::PDE4D2 [pLEV3-AC3]	git2-2::his7+(7)	
CHP1901	-	his7-366	pap1D::ura4- cgs2::PDE4A5 adh::[pLEV3-AC2 LEU2+]	git2-2::his7+(7)	
CHP1919		+	pap1D::ura4- cgs2::PDE8A[LEU2] [pLEV3-AC4-LEU2+]	git2-2::his7+(7)	
CHP1923	+	his7-366	pap1D::ura4- cgs2::PDE4D2 adh::[pLEV3-AC2 LEU2+] ars1[pNMT1-GNAS1R201C LEU2+]	git2-2::his7+(7)	
CHP1925	+	his7-366	pap1D::ura4- cgs2::PDE1B adh::[pLEV3-AC7 LEU2+]	git2-2::his7+(7)	
CHP1927	+	his7-366	pap1D::ura4- cgs2::PDE2A adh::[pLEV3-AC7 LEU2+]	git2-2::his7+(7)	
CHP1928	+	his7-366	pap1D::ura4- cgs2::PDE4B3 adh::[pLEV3-AC7 LEU2+]	git2-2::his7+(7)	
CHP1943	+	?	pap1D::ura4- cgs2::kan-adh1-PDE1C4 [pLEV3-AC2 LEU2+]	git2-2::his7+(7)	
CHP1949	+	?	pap1D::ura4- cgs2::PDEhu4A1 [pLEV3-AC7 LEU2+]	git2-2::his7+(7)	
CHP1952	+	?	pap1D::ura4- cgs2::PDE1C4 [pLEV3-AC7 LEU2+]	git2-2::his7+(7)	
CHP1953	+	?	pap1D::ura4- cgs2::kan-adh1-PDE1C4 lys2-97::pJV1L-exoY[lys2]	git2-2::his7+(7)	
CHP1960	-	+	pap1D::ura4- cgs2::PDE4D2 lys2-97 [pJV1L-AC6:4]	git2-2::his7+(7)	
CHP1963	+	+	pap1D::ura4- cgs2::PDE4D2 lys2-97 [pJV1L-AC6:4] ars1[pNMT1-GNAS1R201C LEU2+]	git2-2::his7+(7)	
CHP2009	+	?	pap1D::ura4- cgs2::PDE4D2 [pLEV3-AC4 LEU2+]	git2-2::his7+(7)	
CHP2023	-	+	pap1D::ura4- cgs2::kan-adh1-PDE1C4 lys2-97 pJV1tif-AC9:4(9)	git2-2::his7+(7)	
CHP2026	-	+	pap1D::ura4- cgs2::PDE4D2 lys2-97 pJV1tif-AC9:4(9)	git2-2::his7+(7)	
CHP2027	+	+	pap1D::ura4- cgs2::PDE4D2 lys2-97 pJV1tif-AC9:4(9) ars1[pNMT1-GNAS1R201C LEU2+]	git2-2::his7+(7)	
CHP2107	-	+	pap1D::ura4- cgs2-2 lys2-97 [pJV1tif-AC9:4(9)] [pLEV3-PDE3Bcat]	git2-2::his7+(7)	
CHP2443	-	+	pap1D::ura4- cgs2::PDE4D2 ars1[pNMT1-GNAS1R201C LEU2+] lys2-97::{pJV1-huAC5m2}	git2-2::his7+(7)	
CHP2445	-	+	pap1D::ura4- cgs2::PDE4D2 ars1[pNMT1-GNAS1R201C LEU2+] lys2-97::{pJV1-huAC5W5:1}	git2-2::his7+(7)	
CHP2486	+	?	pap1D::ura4- cgs2::PDE4D2 lys7-2::pnmt1(lys7)-GNASR201C	git2-2::his7+(7)	
CHP2489	?	?	pap1D::ura4- cgs2::PDE4D2 lys2-97 lys7-2::pnmt1(lys7)-GNASR201C	git2-2::his7+(7)	

All strains carry the *fbp1:GFP* reporter except for CHP731, which still carries *fbp1*, and for CHP1466, which still carries *fbp1:ura4*. All strains carry the *ura4:fbp1-lacZ* reporter except for CHP731, which still carries *ura4*. All strains express *leu1-32*, *ade6*, and *lys1*.

2.1.3 Bacteria

Plasmids (Invitrogen, San Diego) were purified from one of the following strains of *E. coli*: ElectroTen-Blue electroporation-competent cells (Stratagene, La Jolla, CA) or XL-1 Red competent *E. coli* cells (Agilent Technologies, Santa Clara, CA). Transformants were selected for in LB medium containing 100 mg/L ampicillin and incubated at 37℃.

2.1.4 Enzymes

Restriction endonucleases were sustained in buffers provided from the manufacturer (New England Biolabs (NEB), Ipswich, MA). Restriction digestion protocols provided by NEB were followed.

2.1.5 Microscopy

Fluorescence by GFP signal was observed using the EVOS FL with a 4X objective (Life Technologies, Carlsbad, CA) or using an Axioplan 2 microscope with a 40X objective (Zeiss, Jena, Germany). Differential interference contrast (DIC) microscopy was conducted using an Axioplan 2 microscope with a 40X objective (Zeiss, Jena, Germany).

2.2 METHODS

2.2.1 Cyclic Nucleotide Assays

Cultures were grown to exponential phase (5×10^6 to 1.5×10^7 cells/mL) prior to treatment with BCAC compounds together with 40μM Rolipram, and cAMP extracts were prepared and measured by mass spectrometry (Eberhard and Hoffman 2021). Unless otherwise indicated,

cultures were incubated at 30°C with shaking for 30 minutes following treatment with compound, followed by cells being incubated with acetonitrile at room temperature for at least 15 minutes before pelleting.

2.2.2 GFP Assays by Flow Cytometry and Fluorescence-Activated Cell Sorting

Cultures were grown to exponential phase (5×10^6 to 1.5×10^7 cells/mL) to be treated with compound and then incubated overnight following inoculation. Flow cytometry readings were conducted by resuspending cells in PBS and then reading their fluorescent intensity by GFP signal on a FACSAria Illu machine (BDBiosciences, Franklin Lakes, NJ). Sorting of cells by GFP signal was also conducted on this machine, and cells (between 2000- and 10,000-count) fluorescing below a specified fluorescence intensity were collected into 1 mL of liquid EMM and spread onto YES.

2.2.3 Whole-cell PCR

PCR was performed using 2X buffer (Failsafe Buffer G, Lucigen), oligonucleotides, DNA polymerase (Phusion, New England Biolabs) and a small amount (roughly the size of a pin's tip) of cells. Cells were incubated at 98ºC for 10 minutes before entering a standard 40-cycle PCR reaction. PCR product bands were loaded onto 1% agarose gel and visualized with ethidium bromide/UV rays.

2.2.4 Plasmid Rescue from Yeast

Plasmids were rescued from yeast using the Smash and Grab protocol (Hoffman and Winston 1987). Yeast cells were suspended in 0.2 mL of Smash and Grab buffer, prepared as described

by Hoffman and Winston, and then vortexed in the presence of 0.2 mL of phenol-chloroform and 0.3 grams of acid-washed glass beads. Cells were pelleted, and 10 μL of the aqueous layer was added to 40 μL of sterile water. 0.5 μL of this solution was used in *E. coli* transformations.

2.2.5 Transformation of *Escherichia coli*

E. coli transformations used either ElectroTen-Blue electroporation-competent cells (Agilent) or XL-1 Red competent cells (Agilent). For transformation of ElectroTen-Blue cells, cells were electroporated (2250 V/cm, 200 Ohms, 25 microfarad) to achieve a time constant of 4.5 msec. Electroporated cells were collected into 1 mL of S.O.C. broth (2% tryptone, 0.5% yeast extract) (ThermoFisher) and incubated at 37℃ for 1 hour with shaking before being pelleted for 7 minutes at 4000 RPM. The pellet was resuspended in 100 μL of S.O.C. and spread to an LB+Ampicillin plate, which was grown overnight at 37℃. For transformation of XL-1 Red cells, chemically competent cells were mixed with 1.7 μL of β-mercaptoethanol and swirled every 2 minutes for 10 minutes while being kept on ice. 1 μL of 50 ng/μL plasmid DNA was added, and the mixture was incubated on ice for 30 minutes. The mixture was heat-pulsed at 42ºC for 45 seconds before being incubated on ice again for 2 minutes. 0.9 mL of S.O.C. was added, and cells were shaken at 37℃ for 1 hour before being pelleted for 10 minutes at 1000 RPM. The supernatant was poured off, and cells were plated to LB+Ampicillin plates and incubated for two to three days at 37℃.

2.2.6 Plasmid preparations from *Escherichia coli*

Plasmids were prepared from *E. coli* transformed using the QIAprep Spin Miniprep Kit according to the manufacturer's instructions (Qiagen).

2.2.7 Transformation of *Schizosaccharomyces pombe*

Yeast was grown overnight in YES liquid or, for non-AC-carrying strains, in EMM+1μM cAMP+1μM Rolipram. Cultures were grown to exponential phase in EMM (5×10^6 to 1.5×10^7 cells/mL), pelleted for 3 minutes at 4000 RPM, and washed with sterile water to maintain log-phase cell density. Cells were pelleted, resuspended in 1 mL of sterile water, and pelleted for 5 seconds in the microfuge at 14000 RPM. Cells were then washed with 1 mL of 1X LiOAc/TE buffer, pelleted, and brought to 2×10^9 cells/mL in 1X LiOAc/TE. Cells (100 μL) were mixed with 2 μL of 10 mg/mL boiled carrier DNA (salmon sperm) and transforming DNA. The mixture was incubated for 10 minutes at room temperature before adding 260 μL of PLATE buffer (40% PEG, 100 mM LiOAc, 10mM Tris-HCl pH 7.5). Samples were incubated for 2-3 hours at 30℃. Cells received 43 μL of DMSO and were heat-shocked for 5 minutes at 42℃. Transformants were plated to four EMM selection plates that were incubated at 30℃ for several days. Smaller transformations used from 10 to 50 μL of cells, and they followed the same protocol by adjusting the volumes of DNA, PLATE buffer, and DMSO to maintain the same ratios.

3 ANALYSIS OF cAMP PRODUCTION IN THE PRESENCE OF GNAS

3.1 Profiling Several ACs with 5μM BCAC Compounds Suggests Differential Sensitivities

To determine the effect of BCAC compounds on cAMP production, strains carrying a variety of ACs (A2, AC4, AC6, AC7, and AC9) were analyzed in the presence of BCAC compounds and 40μM Rolipram (to inhibit PDEs and thus triggering an increase in cAMP levels to reflect AC activity). The ACs were under the stimulatory effect of mutationally-activated GNAS ($GNAS^{R201C}$). cAMP assays were first conducted with a BCAC compound concentration of 5μM and involved a 30-minute incubation period following inoculation. The fold-elevation of cAMP production was calculated for DMSO vehicle controls and for samples treated with compounds, and the results were compared using a paired t-test (two-tailed) to determine statistical significance. Because the t-test was paired, the magnitude of the difference between the mean fold-elevations of the DMSO controls and those of the compound-treated samples does not fully reflect the variability seen among individual assays. cAMP production was calculated as a fold-elevation as this eliminates fluctuation in the absolute cAMP elevation across experiments, which is a function of cell density ranging between 5×10^6 and 1.5×10^7 cells/mL.

The results are shown for each AC (Tables 3-7, Figures 5-9). The fold-elevations of the DMSO controls tend to range over the compounds tested on each AC, and the cAMP extracted from DMSO controls was sometimes greater than that extracted from compound-treated samples. This is most likely due to variable quality of the growth medium or to strains' varying responses to Rolipram (loss of sensitivity to Rolipram would result in decreased cAMP elevation). The results of experiments were omitted (no more than 3 for each BCAC compound for each strain) that did not show at least a three-fold elevation of cAMP in the DMSO-treated control or a "time=0

minutes" cAMP level greater than that of the DMSO control. This suggested an issue with the culture, such as loss of sensitivity to Rolipram. AC2 experiments with BCAC70, 87-92 are not included, as their results all reflected sub-quality cultures.

Table 3. cAMP Production in CHP1923 (AC2) Following Treatment with 5μM Compounds

BCAC Compound of Treatment (5μM)	Fold-elevation – DMSO controls (mean)	Fold-elevation – DMSO controls (std. dev.)	Fold-elevation – BCAC compound (mean)	Fold-elevation – BCAC compound (std. dev.)	Number of assays
54	6.44	5.62	3.97	0.62	4
61	6.44	5.62	3.55	0.55	4
62	6.44	5.62	2.62	0.41	4
63	6.44	5.62	5.74	0.89	4
66	6.44	5.62	5.71**	0.89	4
67	6.44	5.62	3.22	0.5	4

Statistical significance was calculated as the result of a paired t-test (two-tailed) comparing fold-elevations of DMSO-treated samples with compound-treated ones and is indicated as follows: *=p<.10, **=p<.05, ***=p<.01. cAMP production was calculated as a fold-elevation, according to the following ratio:

$$elevation = \frac{\text{extracted cAMP (units: spectral counts) at T=30 minutes after compound treatment}}{\text{extracted cAMP (units: spectral counts) at time of compound treatment (T=0 minutes)}}.$$

Table 4. cAMP Production in CHP1826 (AC4) Following Treatment with 5μM Compounds

BCAC Compound of Treatment (5uM)	Fold-elevation – DMSO controls (mean)	Fold-elevation – DMSO controls (std. dev.)	Fold-elevation – BCAC compound (mean)	Fold-elevation – BCAC compound (std. dev.)	Number of assays
54	13.07	5.03	2.18**	1.97	9
61	13.07	5.03	1.67***	1.52	9
62	13.39	5.27	1.65***	1.42	8
63	13.07	5.03	0.90***	0.30	9
66	13.07	5.03	2.41***	1.33	9
67	13.07	5.03	1.48***	1.02	9
70	5.14	1.84	4.57	0.88	4
87	5.14	1.84	2.79	0.3	4
88	5.14	1.84	4.68	1.09	4
89	5.14	1.84	4.92	0.95	4
90	5.14	1.84	7.88	8.24	4
91	5.14	1.84	5.1	0.53	4
92	5.14	1.84	6.52	0.79	4

Statistical significance was calculated as described beneath Table 3 and is indicated as follows: *=p<.10, **=p<.05, ***=p<.01. Fold-elevation of cAMP was calculated as described beneath Table 3.

Table 5. cAMP Production in CHP1963 (AC6) Following Treatment with 5μM Compounds

BCAC Compound of Treatment (5uM)	Fold-elevation – DMSO controls (mean)	Fold-elevation – DMSO controls (std. dev.)	Fold-elevation – BCAC compound (mean)	Fold-elevation – BCAC compound (std. dev.)	Number of assays
54	11.65	4.11	6.18*	2.01	5
61	11.65	4.11	5.32***	3.51	5
62	10.62	2.05	5.68**	2.16	5
63	10.62	2.05	4.46***	0.87	5
66	10.62	2.05	5.61**	1.69	5
67	10.62	2.05	5.21**	1.43	5
70	5.03	0.56	4.76	1.67	3
87	5.03	0.56	3.28	2.25	3
88	5.03	0.56	5.06	1.02	3
89	5.03	0.56	4.94	3.79	3
90	5.03	0.56	3.27	1.02	3
91	5.03	0.56	4.72	1.39	3
92	5.03	0.56	5.08	1.54	3

Statistical significance was calculated as described beneath Table 3 and is indicated as follows: *=p<.10, **=p<.05, ***=p<.01.

Fold-elevation of cAMP was calculated as described beneath Table 3.

Table 6. cAMP Production in CHP1817 (AC7) Following Treatment with 5μM Compounds

BCAC Compound of Treatment (5uM)	Fold-elevation – DMSO controls (mean)	Fold-elevation – DMSO controls (std. dev.)	Fold-elevation – BCAC compound (mean)	Fold-elevation – BCAC compound (std. dev.)	Number of assays
54	9.36	3.02	2.03***	1.09	8
61	9.56	3.21	1.68***	1.07	7
62	9.36	3.01	2.25**	1.51	8
63	9.36	3.02	1.30***	0.61	8
66	9.36	3.02	3.01***	1.89	8
67	9.36	3.02	1.78***	0.87	8
70	4.56	0.31	4.32	1.37	3
87	4.56	0.31	3.11	1.17	3
88	4.56	0.31	5.03	1.72	3
89	4.56	0.31	4.52	1.49	3
90	4.56	0.31	4.28	2.99	3
91	4.56	0.31	5.33	2.06	3
92	4.56	0.31	5.72	1.69	3

Statistical significance was calculated as described beneath Table 3 and is indicated as follows: *=p<.10, **=p<.05, ***=p<.01.

Fold-elevation of cAMP was calculated as described beneath Table 3.

Table 7. cAMP Production in CHP2027 (AC9) Following Treatment with 5μM Compounds

BCAC Compound of Treatment (5uM)	Fold-elevation – DMSO controls (mean)	Fold-elevation – DMSO controls (std. dev.)	Fold-elevation – BCAC compound (mean)	Fold-elevation – BCAC compound (std. dev.)	Number of assays
54	11.79	6.88	5.52	4.12	5
61	11.79	6.88	2.85**	1.11	5
62	11.79	6.88	7.43	4.11	5
63	11.79	6.88	3.71**	1.45	5
66	11.79	6.88	7.49	2.95	5
67	11.79	6.88	5.42*	3.21	5
70	7.62	0.24	4.63	0.46	2
87	7.62	0.24	8.72	7.53	2
88	7.62	0.24	7.60	2.11	2
89	7.62	0.24	13.94	9.19	2
90	7.62	0.24	4.49	0	2
91	7.62	0.24	6.51	1.98	2
92	7.62	0.24	6.30	0.53	2

Statistical significance was calculated as described beneath Table 3 and is indicated as follows: *=p<.10, **=p<.05, ***=p<.01. Fold-elevation of cAMP was calculated as described beneath Table 3.

Figure 5. CHP1923 (AC2) was treated with 5μM BCAC compounds and DMSO as a control (plus 40μM Rolipram), and cAMP production was measured by mass spectrometry before and after a 30-minute incubation period following inoculation with compounds. Statistical significance was calculated as described beneath Table 3 and is indicated as follows: *=p<.10, **=p<.05, ***=p<.01. Fold-elevation of cAMP was calculated as described beneath Table 3. Mean fold-elevation was calculated for all the experiments done with each compound, and the error bars represent the standard deviation.

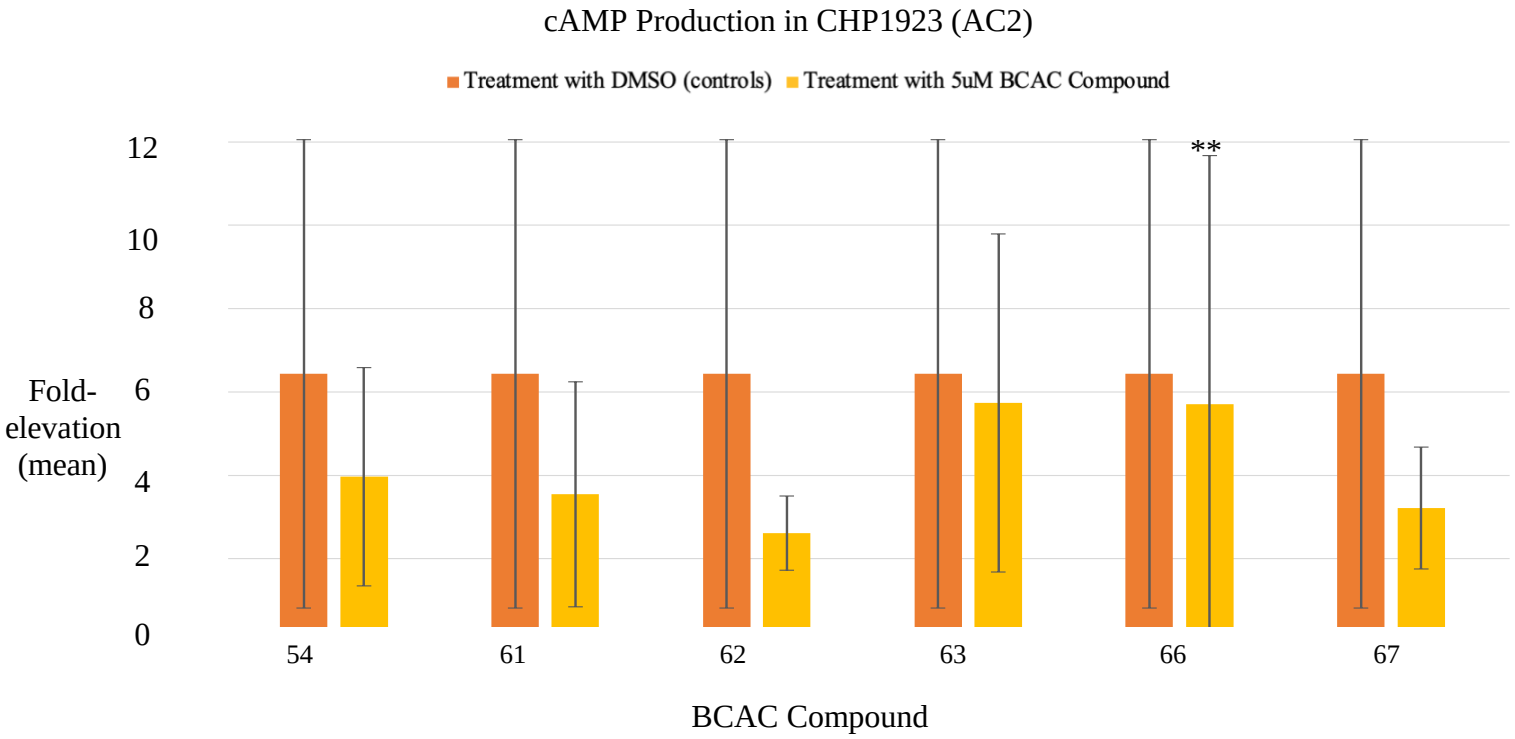

Figure 6. CHP1826 (AC4) was treated with 5μM BCAC compounds and DMSO as a control (plus 40μM Rolipram), and cAMP production was measured by mass spectrometry before and after a 30-minute incubation period following inoculation with compounds. Statistical significance was calculated as described beneath Table 3 and is indicated as follows: *=p<.10, **=p<.05, ***=p<.01. Fold-elevation of cAMP was calculated as described beneath Table 3. Mean fold-elevation was calculated for all the experiments done with each compound, and the error bars represent the standard deviation.

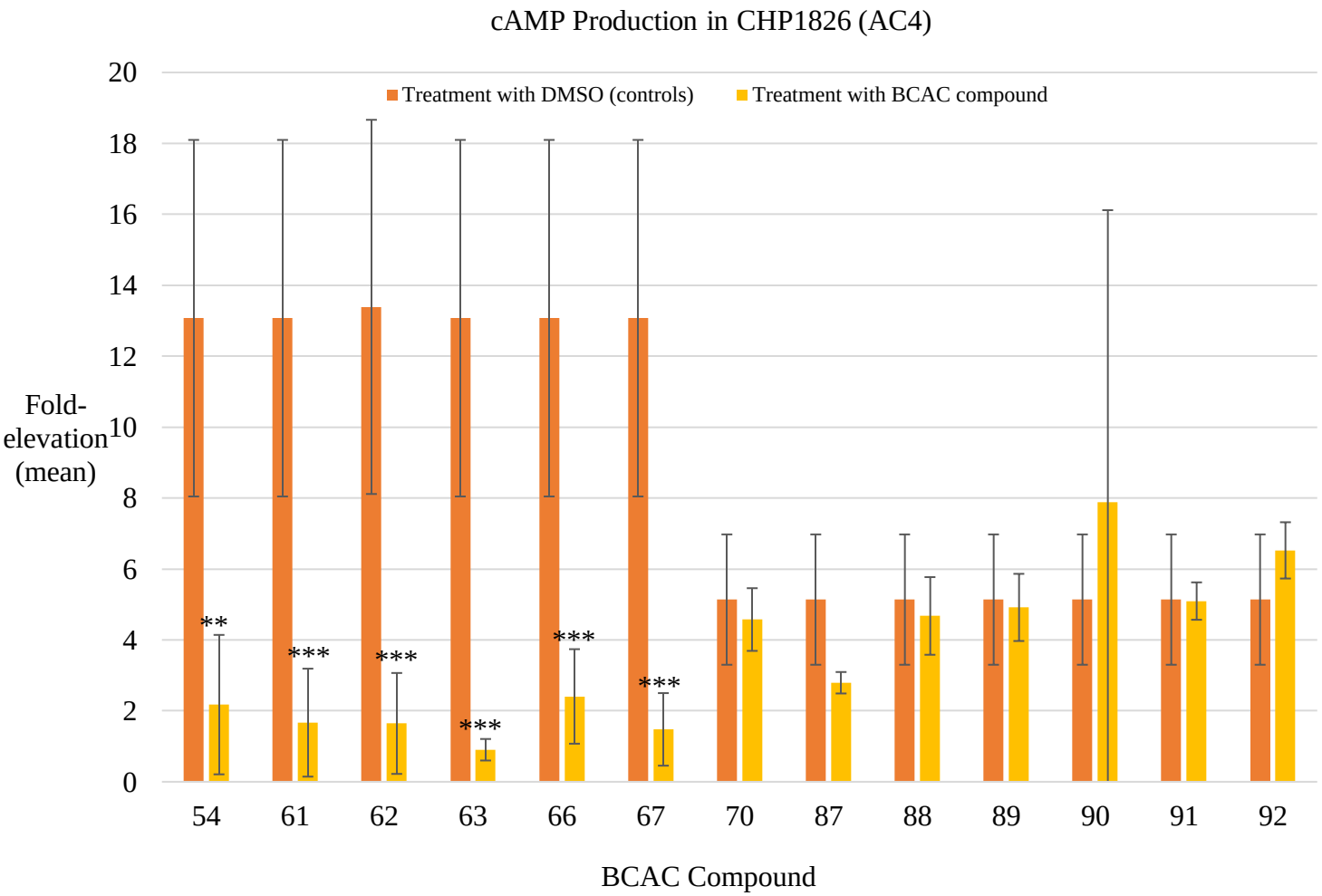

Figure 7. CHP1963 (AC6) was treated with 5μM BCAC compounds and DMSO as a control (plus 40μM Rolipram), and cAMP production was measured by mass spectrometry before and after a 30-minute incubation period following inoculation with compounds. Statistical significance was calculated as described beneath Table 3 and is indicated as follows: *=p<.10, **=p<.05, ***=p<.01. Fold-elevation of cAMP was calculated as described beneath Table 3. Mean fold-elevation was calculated for all the experiments done with each compound, and the error bars represent the standard deviation.

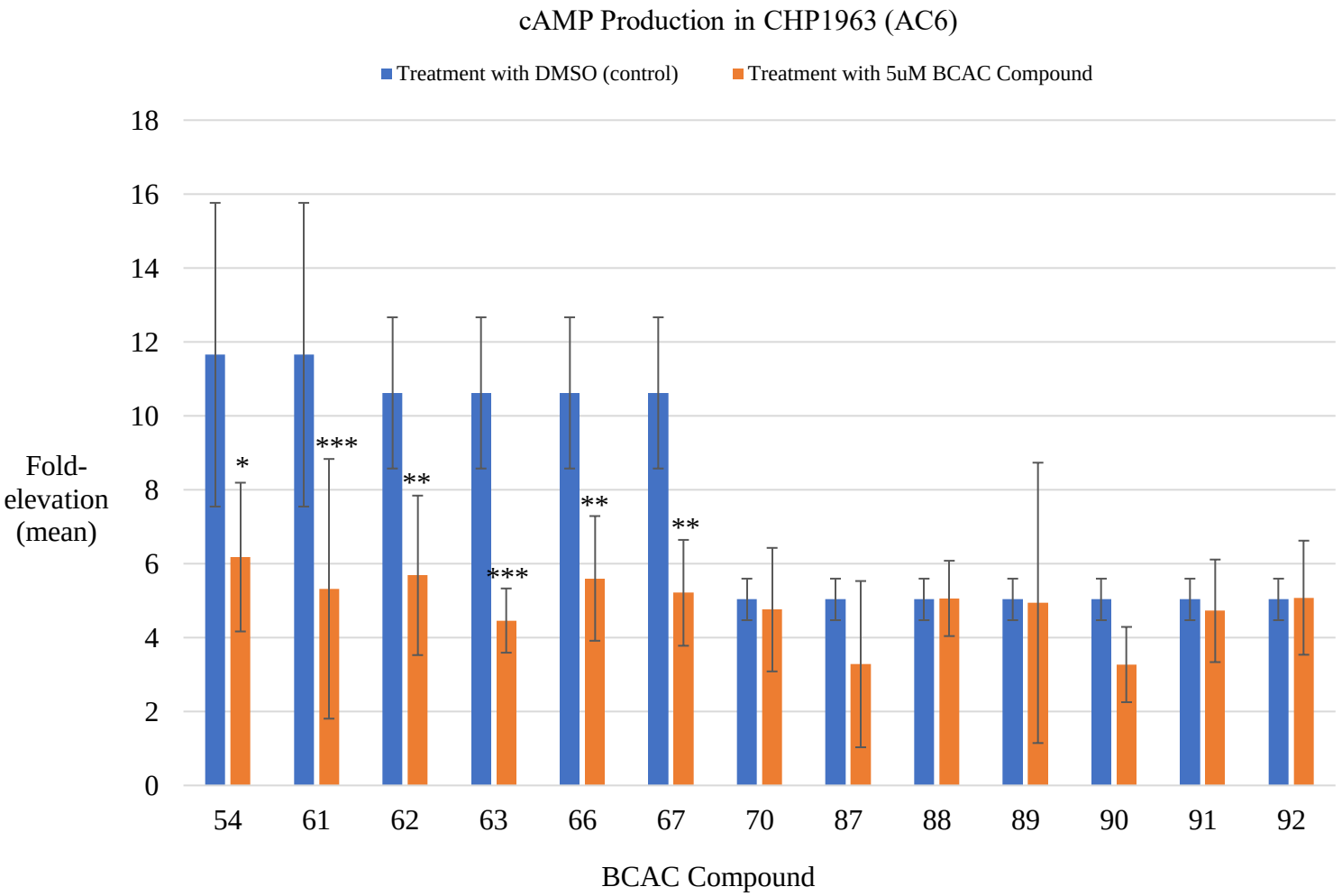

Figure 8. CHP1817 (AC7) was treated with 5μM BCAC compounds and DMSO as a control (plus 40μM Rolipram), and cAMP production was measured by mass spectrometry before and after a 30-minute incubation period following inoculation with compounds. Statistical significance was calculated as described beneath Table 3 and is indicated as follows: *=p<.10, **=p<.05, ***=p<.01. Fold-elevation of cAMP was calculated as described beneath Table 3. Mean fold-elevation was calculated for all the experiments done with each compound, and the error bars represent the standard deviation.

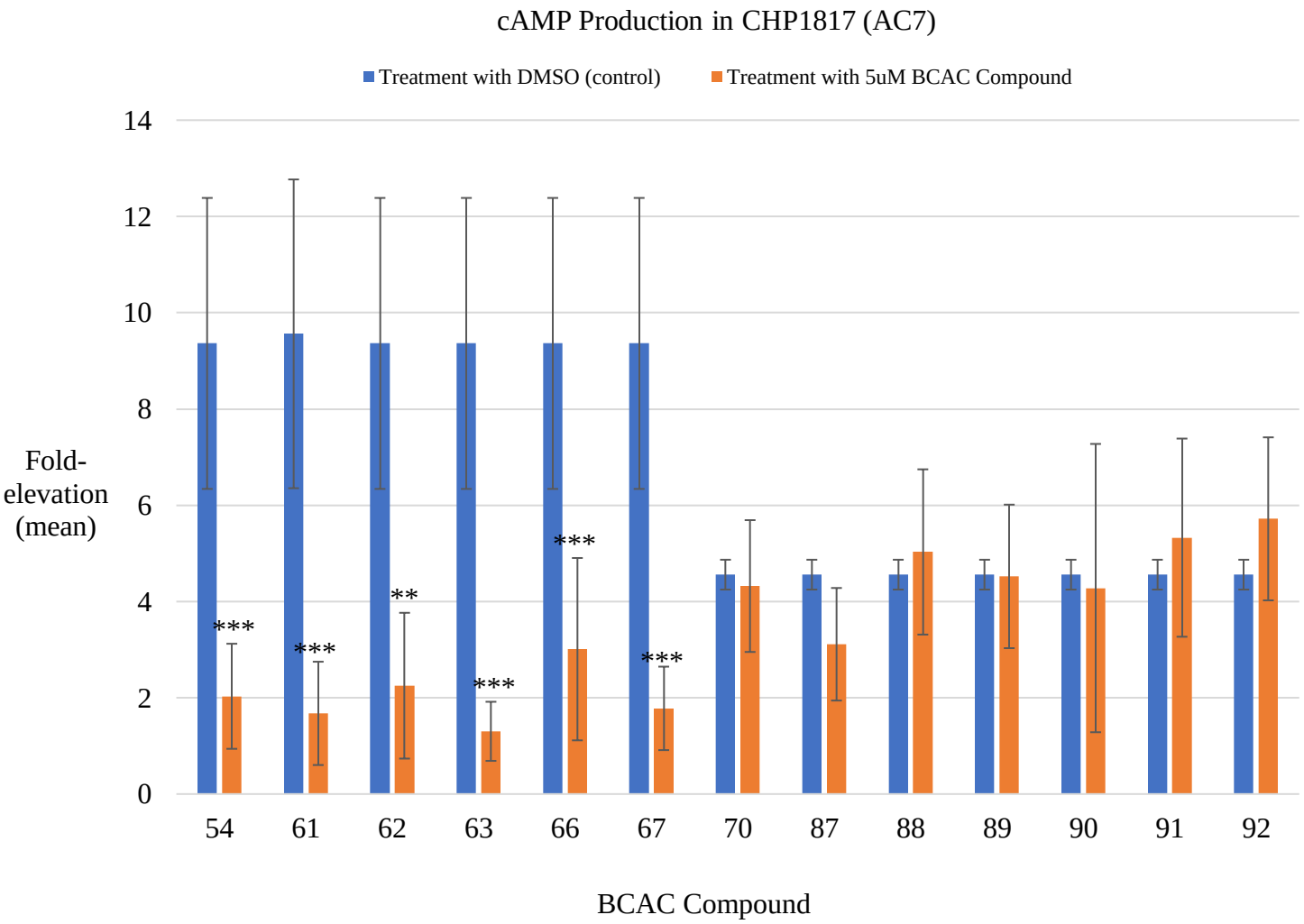

Figure 9. CHP2027 (AC9) was treated with 5μM BCAC compounds and DMSO as a control (plus 40μM Rolipram), and cAMP production was measured by mass spectrometry before and after a 30-minute incubation period following inoculation with compounds. Statistical significance was calculated as described beneath Table 3 and is indicated as follows: *=p<.10, **=p<.05, ***=p<.01. Fold-elevation of cAMP was calculated as described beneath Table 3. Mean fold-elevation was calculated for all the experiments done with each compound, and the error bars represent the standard deviation.

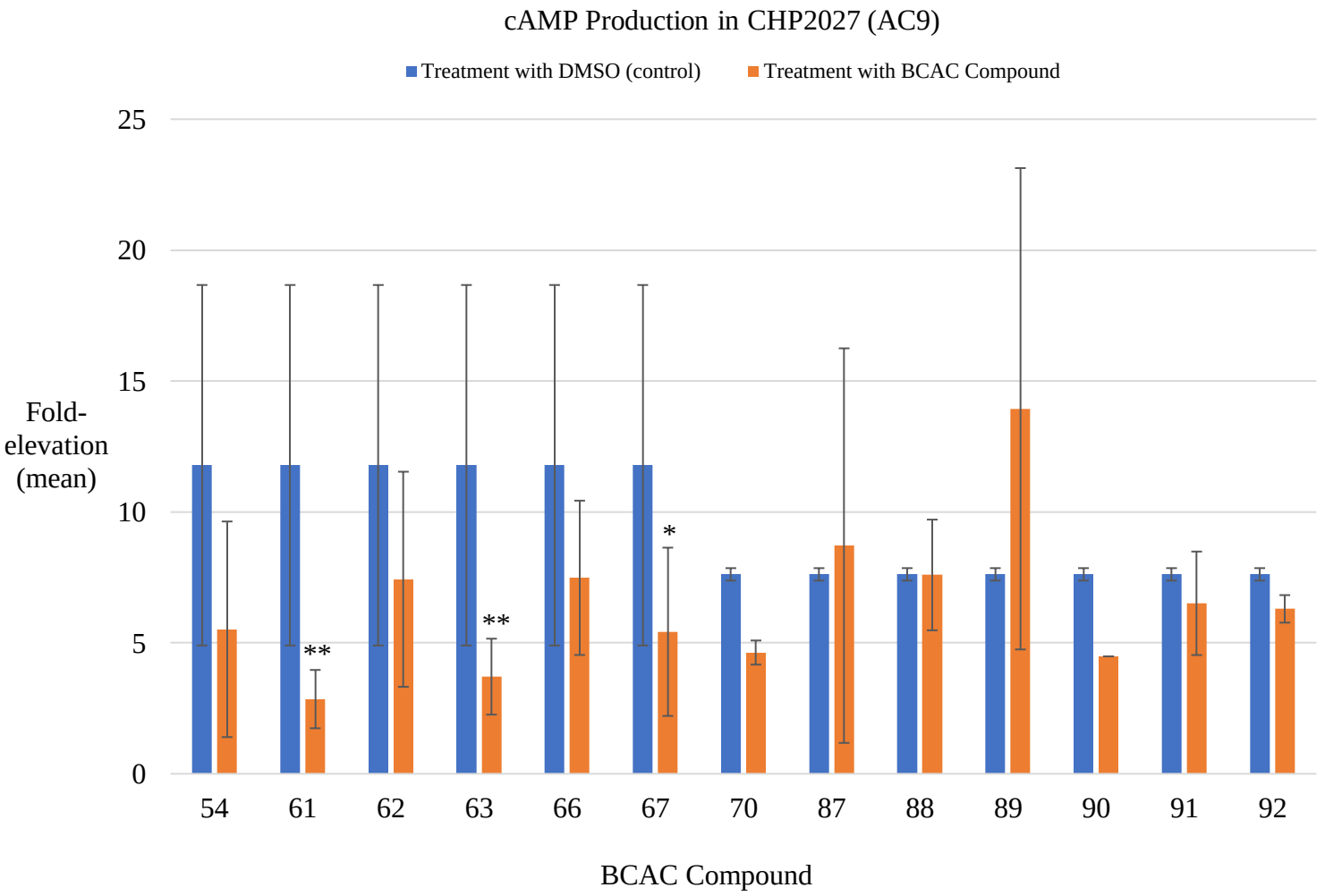

3.2 AC Profiling with Lower BCAC Concentrations Also Suggests Different Sensitivities

In an effort to profile all 41 members of the BCAC51 scaffold of compounds, we conducted cAMP assays on strains expressing AC4, AC5, and AC7, as these ACs seemed to show the greatest sensitivity to the compounds at 5μM. The strains also expressed mutationally-activated GNAS ($GNAS^{R201C}$) to stimulate the ACs. Strains were treated with lower concentrations of BCAC compounds in an effort to reduce any effect of cell growth arrest; due to the lower concentrations being used, the incubation time for cultures after inoculation was increased to 60 minutes to maximize the amount of cAMP extracted. The fold-elevation of cAMP production was calculated for samples treated with DMSO as a vehicle control and for those treated with compounds, and the mean results for experiments done on each compound for all ACs are shown (Tables 8-10, Figures 10-12). The average ratio of fold-elevation for compound-treated sample to fold-elevation for DMSO-treated control was also calculated (Tables 8-10). Experiments were conducted with sets of compounds at both 2.5μM and 1.25μM (plus 40μM Rolipram) with each set having its own DMSO control. Between 3 and 6 assays were completed with each set. Again, the fold-elevations of the DMSO controls tended to range over the compounds tested on each AC-expressing strain, and the cAMP extracted from DMSO controls was sometimes greater than that extracted from compound-treated samples. This is most likely due to variable quality of the cell growth and loss of sensitivity to Rolipram. The results of 1 of the 3 experiments on AC4 were omitted from the calculations, as they did not show at least a three-fold elevation of cAMP in the DMSO-treated control or a “time=0 minutes” cAMP level greater than that of the DMSO control. This suggested an issue with the culture, such as loss of sensitivity to Rolipram or irregular growth medium. Due to the high volume of data generated for many BCAC compounds, the results for any compound that did not reduce the fold-elevation of cAMP to at

least 60% that of the DMSO-treated sample (indicated by a fold-elevation ratio of less than .60) were omitted.

Table 8. cAMP Production in CHP1826 (AC4) Following Treatment with Sets of BCAC Compounds at 2.5μM and 1.25μM

	BCAC compound #, Concentration	Fold-elevation (mean)	Std. dev. of fold-elevation	Fold-elevation ratio (mean)
Set 1	DMSO	5.01	0.64	
	51 2.5μM	1.77***	0.74	0.19
	51 1.25 μM	2.55***	0.61	0.39
	52 2.5 μM	1.67**	1.06	0.17
	52 1.25μM	2.03**	0.77	0.26
	53 2.5μM	1.70***	0.85	0.18
	53 1.25μM	1.46***	0.17	0.11
	54 2.5μM	0.91***	0.29	-0.02
	54 1.25μM	1.99**	1.17	0.25
Set 2	DMSO	8.15	5.24	
	57 2.5μM	4.98	2.62	0.56
	57 1.25μM	6.48	3.37	0.77
	61 2.5μM	2.06	0.14	0.15
	61 1.25μM	6.52**	2.48	0.77
	62 2.5μM	4.70	1.36	0.52
	62 1.25μM	3.60***	2.57	0.36
	63 2.5μM	2.54	0.82	0.22
	63 1.25μM	4.02***	2.68	0.42
Set 3	DMSO	8.96	3.95	
	64 2.5μM	5.92	4.19	0.62
	64 1.25μM	5.16	4.94	0.52
	65 2.5μM	4.35*	1.53	0.42
	65 1.25μM	13.00	9.21	1.51
	66 2.5μM	3.49	1.16	0.31
	66 1.25μM	6.99	3.46	0.75
	67 2.5μM	4.84	1.33	0.48
	67 1.25μM	2.10	0.73	0.14
Set 4	DMSO	9.43	3.73	
	88 2.5μM	12.00	13.08	1.31
	88 1.25μM	12.82	12.55	1.4
	89 2.5μM	5.39	0.63	0.52
	89 1.25μM	4.33	0.78	0.4
	90 2.5μM	5.62	2.44	0.55
	90 1.25μM	11.38	6.36	1.23
Set 5	DMSO	10.53	5.02	
	91 2.5μM	6.31	2.89	0.56
	91 1.25μM	11.15	1.5	1.06
	92 2.5μM	5.80	2.23	0.5
	92 1.25μM	7.16	3.33	0.65
	93 2.5μM	8.17	2.49	0.75
	93 1.25μM	10.59	6.95	1.01
	94 2.5μM	7.87	1.96	0.72
	94 1.25μM	6.98	5.21	0.63
Set 6	DMSO	6.24	2.95	
	99 2.5μM	3.61**	2.27	0.5
	99 1.25μM	3.82**	1.86	0.54
	101 2.5μM	5.74	0.59	0.91
	101 1.25μM	7.08	1.01	1.16
Set 7	DMSO	5.86	2.05	
	103 2.5μM	4.00	1.14	0.62
	103 1.25μM	4.05	0.79	0.63
	104 2.5μM	3.12*	1.33	0.44
	104 1.25μM	3.87	1.16	0.59
	105 2.5μM	2.48**	0.25	0.3
	105 1.25μM	3.68*	0.98	0.55
Set 8	DMSO	5.63	2.83	
	108 2.5μM	2.77	1.08	0.38
	108 1.25μM	3.80	1.8	0.61
	109 2.5μM	2.80	1.65	0.39
	109 1.25μM	4.60	2.83	0.78
	110 2.5μM	2.26*	1.08	0.27
	110 1.25μM	2.91	1.17	0.41
	111 2.5μM	1.86*	1.06	0.19
	111 1.25μM	3.07	1.72	0.45
	111 2.5μM	2.31*	1.04	0.21
	111 1.25μM	3.95	1.17	0.47

Fold-elevation of cAMP was calculated as follows:

$$elevation = \frac{\text{extracted cAMP (units: spectral counts) at T=60 minutes after compound treatment}}{\text{extracted cAMP (units: spectral counts) at time of compound treatment (T=0 minutes)}}.$$

Statistical significance was calculated by comparing the fold-elevations of DMSO-treated samples with compound-treated ones (paired t-test, two-tailed) and is indicated as follows: *=p<.10, **=p<.05, ***=p<.01. The fold-elevation ratio was calculated as $\frac{(\text{cAMP fold-elevation for comound-treated sample}-1)}{(\text{cAMP fold-elevation for DMSO-treated control}-1)}$.

Table 9. cAMP Production in CHP2445 (AC5) Following Treatment with Sets of BCAC Compounds at 2.5μM and 1.25μM

	BCAC compound #, Concentration	Fold-elevation (mean)	Std. dev. of fold-elevation	Fold-elevation ratio (mean)
Set 1	DMSO	24.47	15.85	
	51 2.5μM	16.67**	10.84	0.67
	51 1.25 μM	18.98*	12.06	0.77
	52 2.5 μM	17.67	11.86	0.71
	52 1.25μM	20.86	4.23	0.85
	53 2.5μM	14**	7.64	0.55
	53 1.25μM	14.11**	7.83	0.56
	54 2.5μM	19.15	9.43	0.77
	54 1.25μM	31.4	19.61	1.3
	57 2.5μM	14.76	5.69	0.59
	57 1.25μM	25.02	13.5	1.02
Set 2	DMSO	17.27	8.65	
	61 2.5μM	6.14**	3.15	0.32
	61 1.25μM	13.17	5.43	0.75
	62 2.5μM	9.47**	7.28	0.52
	62 1.25μM	12.23	4.44	0.69
	63 2.5μM	8.69*	3.99	0.47
	63 1.25μM	13.12	5.9	0.74
	64 2.5μM	23.81	6.67	1.4
	64 1.25μM	19.26	4.69	1.12
	65 2.5μM	12.06	1.02	0.68
	65 1.25μM	10.48	2.84	0.58
Set 3	DMSO	13.83	1.38	
	66 2.5μM	18.54	2.54	1.37
	66 1.25μM	15.1	5.06	1.1
	67 2.5μM	12.06	1.41	0.86
	67 1.25μM	16.07	6.29	1.17
Set 4	DMSO	25.42	ND	
	88 2.5μM	14.65	ND	0.56
	88 1.25μM	19.97	ND	0.78
	89 2.5μM	19.47	ND	0.76
	89 1.25μM	28.82	ND	1.14
	90 2.5μM	20.42	ND	0.8
	90 1.25μM	21.12	ND	0.82
Set 5	DMSO	25.42	ND	
	91 2.5μM	26.98	ND	1.06
	91 1.25μM	11.48	ND	0.43
	92 2.5μM	15.78	ND	0.61
	92 1.25μM	10.13	ND	0.37
Set 6	DMSO	26.94	19.15	
	99 2.5μM	18.85	14.59	0.69
	99 1.25μM	19.81	15.06	0.73
	101 2.5μM	15.96	ND	0.58
	101 1.25μM	15.52	ND	0.56
	103 2.5μM	12.16	ND	0.43
	103 1.25μM	16.54	ND	0.6
	104 2.5μM	14.42	ND	0.52
	104 1.25μM	7.27	ND	0.24
	105 2.5μM	6.11	ND	0.2
	105 1.25μM	9.09	ND	0.31
Set 7	DMSO	26.73	19.32	
	108 2.5μM	22.23	ND	0.83
	108 1.25μM	25.28	ND	0.94
	109 2.5μM	21.67	ND	0.8
	109 1.25μM	26.1	ND	0.98
	110 2.5μM	20.56	ND	0.76
	110 1.25μM	30	ND	1.13
	111 2.5μM	23.81	ND	0.89
	111 1.25μM	17.52	ND	0.64

Statistical significance was calculated as described beneath Table 8 and is indicated as follows: *=$p<.10$, **=$p<.05$, ***=$p<.01$. Fold-elevation of cAMP and the fold-elevation ratio were calculated as described beneath Table 8. Compounds for which standard deviations were not determined are indicated with "ND."

Table 10. cAMP Production in CHP1817 (AC7) Following Treatment with Sets of BCAC Compounds at 2.5μM and 1.25μM

	BCAC compound #, Concentration	Fold-elevation (mean)	Std. dev. of fold-elevation	Fold-elevation ratio (mean)
Set 1	DMSO	17.15	9.55	
	51 2.5μM	17.66	7.91	1.03
	51 1.25 μM	5.73	2.26	0.29
	52 2.5 μM	6.85	3.02	0.36
	52 1.25μM	8.98	3.08	0.49
	53 2.5μM	4.07	1.77	0.19
	53 1.25μM	5.95	3.76	0.31
	54 2.5μM	9.58	3.83	0.53
	54 1.25μM	11.99*	6.66	0.68
Set 2	DMSO	13.43	1.34	
	57 2.5μM	3.5***	0.73	0.2
	57 1.25μM	11.34	2.42	0.83
	61 2.5μM	3.98***	0.91	0.24
	61 1.25μM	5.37	2.66	0.35
	62 2.5μM	6.19**	0.04	0.42
	62 1.25μM	8.06**	1.53	0.57
	63 2.5μM	6.71***	1.66	0.46
	63 1.25μM	7.81**	2.45	0.55
Set 3	DMSO	13.87	5.32	
	64 2.5μM	11.74	4.33	0.83
	64 1.25μM	10.03*	0.43	0.7
	65 2.5μM	7.32	0.52	0.49
	65 1.25μM	11.25	3.25	0.8
	66 2.5μM	9.7	3.39	0.68
	66 1.25μM	10.69	4.18	0.75
	67 2.5μM	10.22	4.26	0.72
	67 1.25μM	8.43	0.65	0.58
Set 4	DMSO	13.34	5.76	
	88 2.5μM	11.01*	4.64	0.85
	88 1.25μM	11.45	6.01	1.04
	89 2.5μM	13.84	5.85	0.55
	89 1.25μM	7.81	6.16	0.85
	90 2.5μM	11.46**	5.37	0.8
	90 1.25μM	10.87	6.35	0.85
Set 5	DMSO	11.67	7.73	
	91 2.5μM	11.55	2.38	0.99
	91 1.25μM	11.72	3.2	1
	92 2.5μM	10.5	1.17	0.89
	92 1.25μM	11.44	4.21	0.98
	93 2.5μM	11.35	3.33	0.97
	93 1.25μM	10.26	4.84	0.87
	94 2.5μM	12.71	3.84	1.1
	94 1.25μM	11.62	5.05	1
Set 6	DMSO	6.81	2.88	
	99 2.5μM	2.44	1.86	0.25
	99 1.25μM	3.87	1.76	0.49
	101 2.5μM	3.51	0.83	0.43
	101 1.25μM	4.96	1.11	0.68
Set 7	DMSO	6.21	2.82	
	103 2.5μM	3.51**	2.1	0.48
	103 1.25μM	5.95	3.24	0.95
	104 2.5μM	4.16	5.26	0.61
	104 1.25μM	4.95	3.01	0.76
	105 2.5μM	2.3*	1.04	0.25
	105 1.25μM	3.31	1.2	0.44
Set 8	DMSO	8.64	2.77	
	108 2.5μM	3.52	1.27	0.33
	108 1.25μM	4.4	0.38	0.44
	109 2.5μM	5.02*	4.5	0.53
	109 1.25μM	3.18*	2.86	0.29
	110 2.5μM	1.87	1.81	0.11
	110 1.25μM	6.29	4.1	0.69
	111 2.5μM	2.08***	1.68	0.14
	111 1.25μM	2.12***	1.76	0.15

Statistical significance was calculated as described beneath Table 8 and is indicated as follows: *=p<.10, **=p<.05, ***=p<.01. Fold-elevation of cAMP and the fold-elevation ratio were calculated as described beneath Table 8.

Figure 10. cAMP assays were conducted on CHP1826 (AC4). Cultures were treated with either 2.5μM or 1.25μM BCAC compound and DMSO vehicle controls (plus 40μM Rolipram), and they were incubated for 1 hour following inoculation. Fold-elevation of cAMP was calculated as described beneath Table 8. The mean fold-elevation is graphed, and the standard deviation is represented by the error bars. Statistical significance was calculated as described beneath Table 8 and is indicated as follows: *=p<.10, **=p<.05, ***=p<.01.

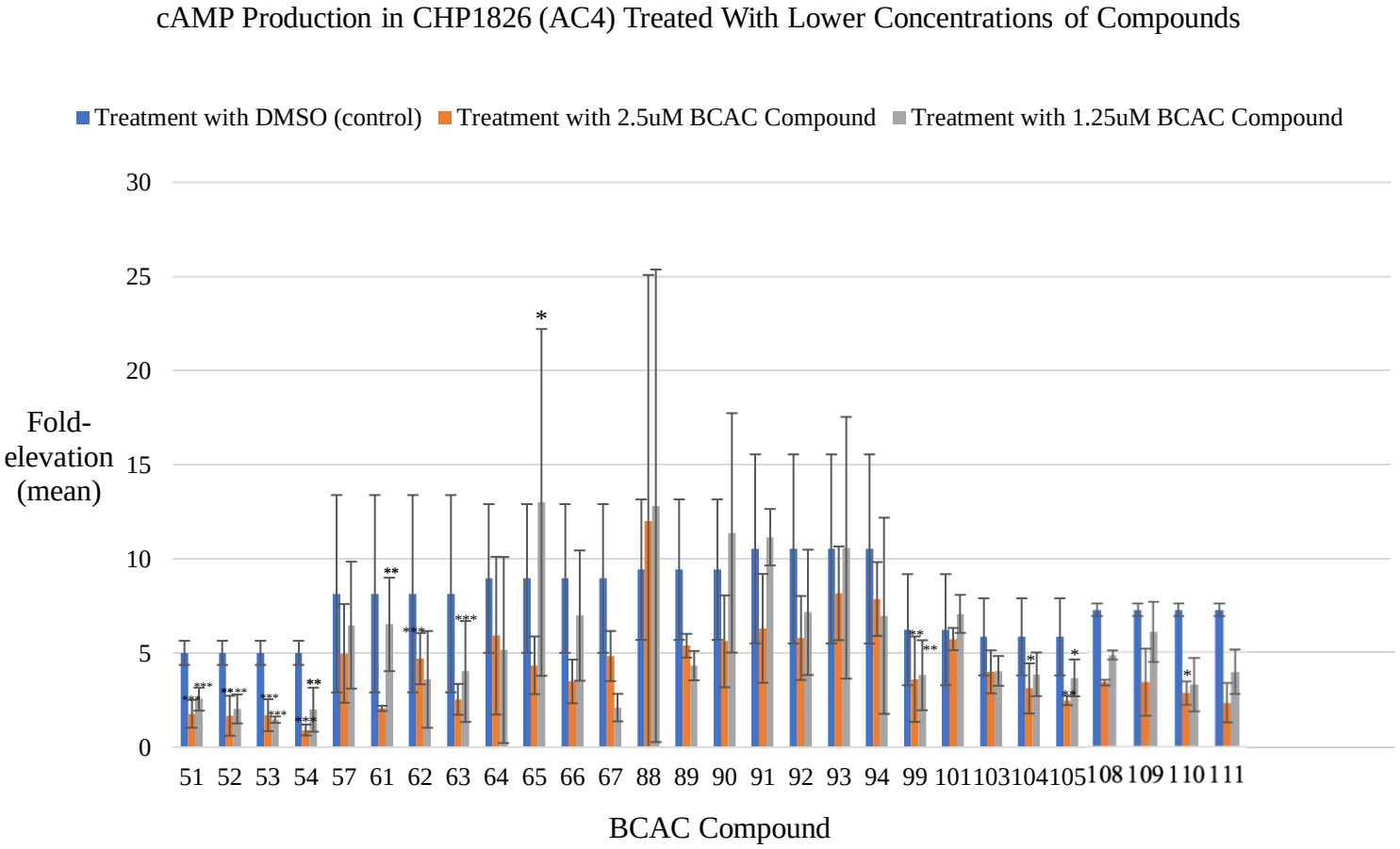

Figure 11. cAMP assays were conducted on CHP2445 (AC5). Cultures were treated with either 2.5μM or 1.25μM BCAC compound and DMSO vehicle controls (plus 40μM Rolipram), and they were incubated for 1 hour following inoculation. Fold-elevation of cAMP was calculated as described beneath Table 8. The mean fold-elevation is graphed, and the standard deviation is represented by the error bars. Statistical significance was calculated as described beneath Table 8 and is indicated as follows: *=p<.10, **=p<.05, ***=p<.01.

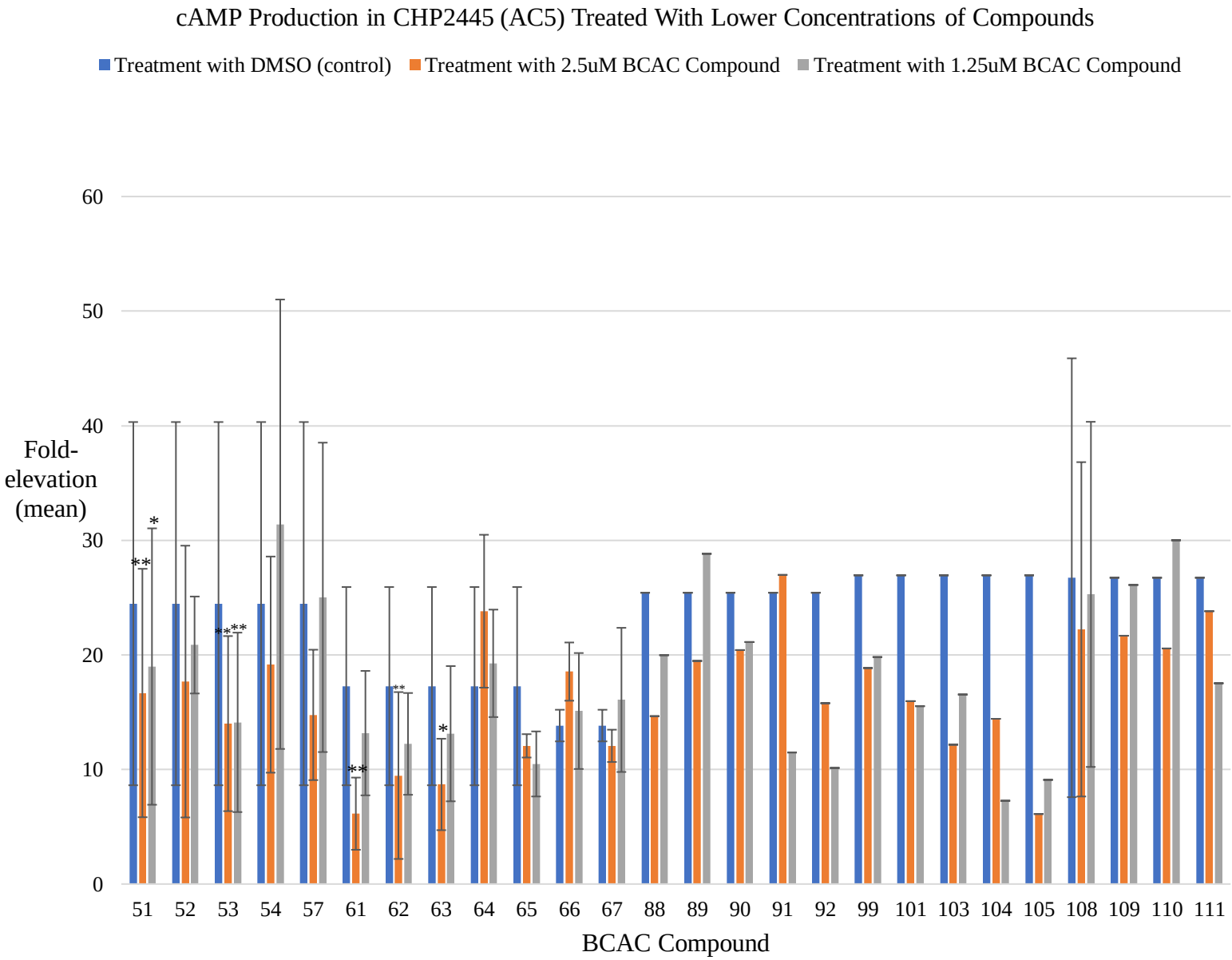

Figure 12. cAMP assays were conducted on CHP1817 (AC7). Cultures were treated with either 2.5μM or 1.25μM BCAC compound and DMSO vehicle controls (plus 40μM Rolipram), and they were incubated for 1 hour following inoculation. Fold-elevation of cAMP was calculated as described beneath Table 8. The mean fold-elevation is graphed, and the standard deviation is represented by the error bars. Statistical significance was calculated as described beneath Table 8 and is indicated as follows: *=p<.10, **=p<.05, ***=p<.01.

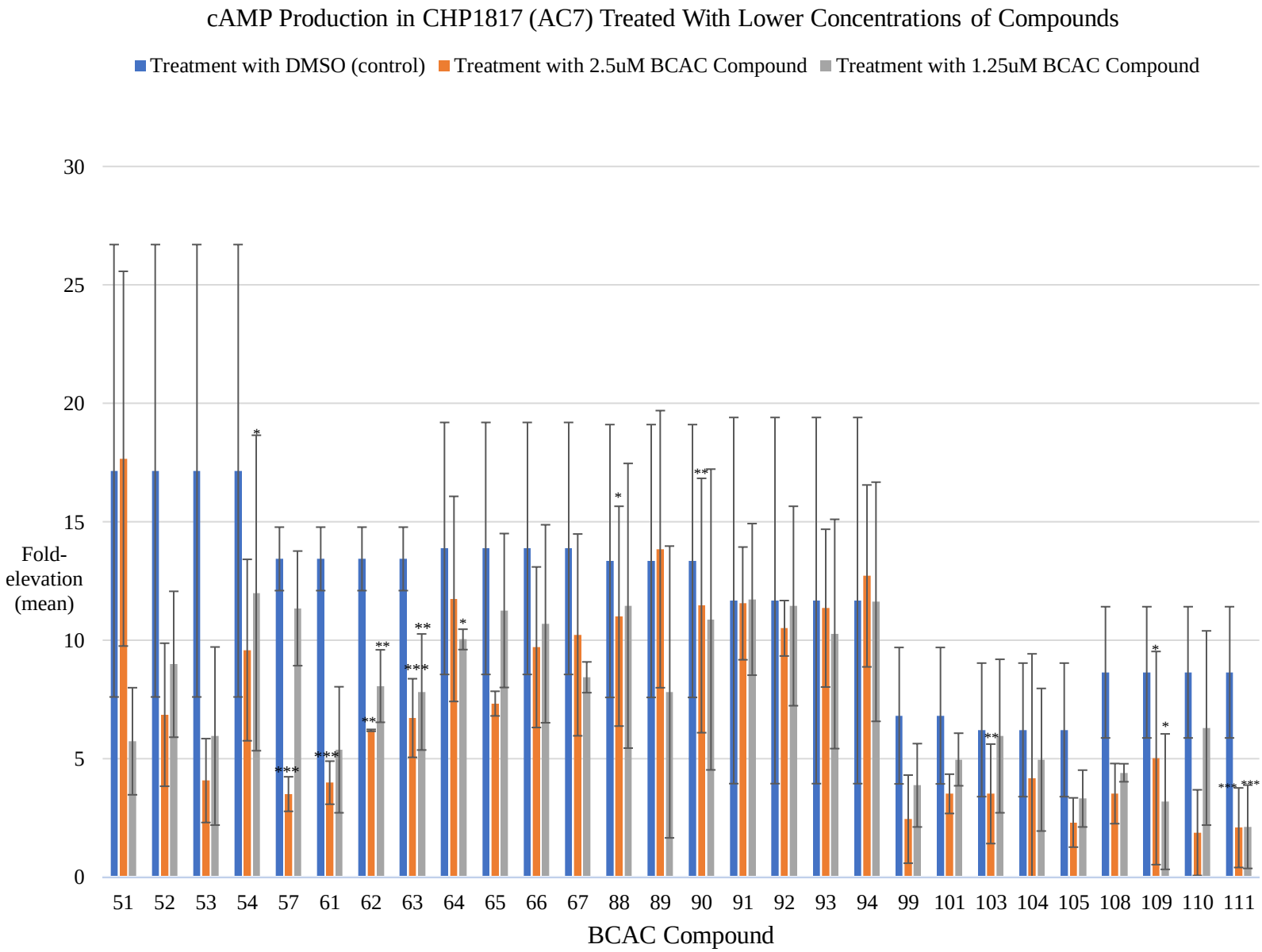

In an attempt to increase the likelihood of observing specificity of compound effect on certain ACs, further assays were carried out with the most active compounds at 1.25μM (plus 40μM Rolipram) on strains expressing AC4, 5, and 9. These experiments included a 30-minute incubation period, since there was no longer a concern about the level of cAMP being extracted. The fold-elevation of cAMP production was calculated for samples treated with DMSO as a vehicle control and for those treated with compounds, and the mean results are shown (Tables 11-13, Figures 13-15). The average ratio of fold-elevation for compound-treated sample to fold-elevation for DMSO-treated control was also calculated (Tables 11-13). Between 6 and 9 assays were done for each compound on each strain. The results of some experiments did not show at least a 3-fold elevation of cAMP in the DMSO-treated control or showed the "time=0 minutes" read as having the highest amount of cAMP, suggesting an issue with the cultures (such as loss of sensitivity to Rolipram). Therefore, these results were not included in the calculations, and this resulted in the elimination of no more than 2 experiments for each strain.

Table 11. cAMP Production in CHP1826 (AC4) Following Treatment with BCAC Compounds at 1.25μM

BCAC Compound of Treatment (5uM)	Fold-elevation (mean)	Fold-elevation (std. dev.)	Fold-elevation ratio
DMSO	7.84	3.98	--
51	3.67**	2.24	0.4
52	4.85*	3.64	0.55
53	3.06**	2.94	0.31
54	5.42***	3.18	0.65
61	3.17**	1.33	0.3
62	4.23**	2.85	0.47
63	4.98***	3.67	0.59
99	4.04**	3.04	0.46
105	3.48**	2.64	0.37

Fold-elevation of cAMP and the fold-elevation ratio were calculated as described beneath Table 8, except extracts were obtained at T=30 minutes rather than at T=60 minutes.

Statistical significance was calculated as described beneath Table 8 and is indicated as follows: *=p<.10, **=p<.05, ***=p<.01.

Table 12. cAMP Production in CHP1963 (AC6) Following Treatment with BCAC Compounds at 1.25μM

BCAC Compound of Treatment (5uM)	Fold-elevation (mean)	Fold-elevation (std. dev.)	Fold-elevation ratio
DMSO	12.22	8.13	--
51	7.41**	5.9	0.58
52	7.23**	7.13	0.55
53	4.75***	4	0.34
54	6.86**	5.85	0.52
61	9.46	6.47	0.75
62	5.52**	3.33	0.4
63	7.1*	5.3	0.55
99	8.35**	6.85	0.65
105	5.36***	4.74	0.38

Fold-elevation of cAMP and the fold-elevation ratio were calculated as described beneath Table 8, except extracts were obtained at T=30 minutes rather than at T=60 minutes.

Statistical significance was calculated as described beneath Table 8 and is indicated as follows: *=p<.10, **=p<.05, ***=p<.01.

Table 13. cAMP Production in CHP2027 (AC9) Following Treatment with BCAC Compounds at 1.25μM

BCAC Compound of Treatment (5uM)	Fold-elevation (mean)	Fold-elevation (std. dev.)	Fold-elevation ratio
DMSO	5.25	3.02	--
51	3.14**	1.69	0.5
52	2.71**	1.83	0.39
53	3.89	2.37	0.67
54	2.39**	1.6	0.34
61	5.25	5.42	1.01
62	4.36	2.68	0.8
63	3.35	2.84	0.56
99	4.7	2.56	0.85
105	4.08	1.82	0.7

Fold-elevation of cAMP and the fold-elevation ratio were calculated as described beneath Table 8, except extracts were obtained at T=30 minutes rather than at T=60 minutes.

Statistical significance was calculated as described beneath Table 8 and is indicated as follows: *=$p<.10$, **=$p<.05$, ***=$p<.01$.

Figure 13. cAMP assays were conducted on CHP1826 (AC4). Cultures were treated with 1.25μM BCAC compound and DMSO vehicle controls (plus 40μM Rolipram), and they were incubated for 30 minutes following inoculation. Fold-elevation of cAMP was calculated as described beneath Table 8. The mean fold-elevation is graphed, and the standard deviation is represented by the error bars. Statistical significance was calculated as described beneath Table 8 and is indicated as follows: *=p<.10, **=p<.05, ***=p<.01.

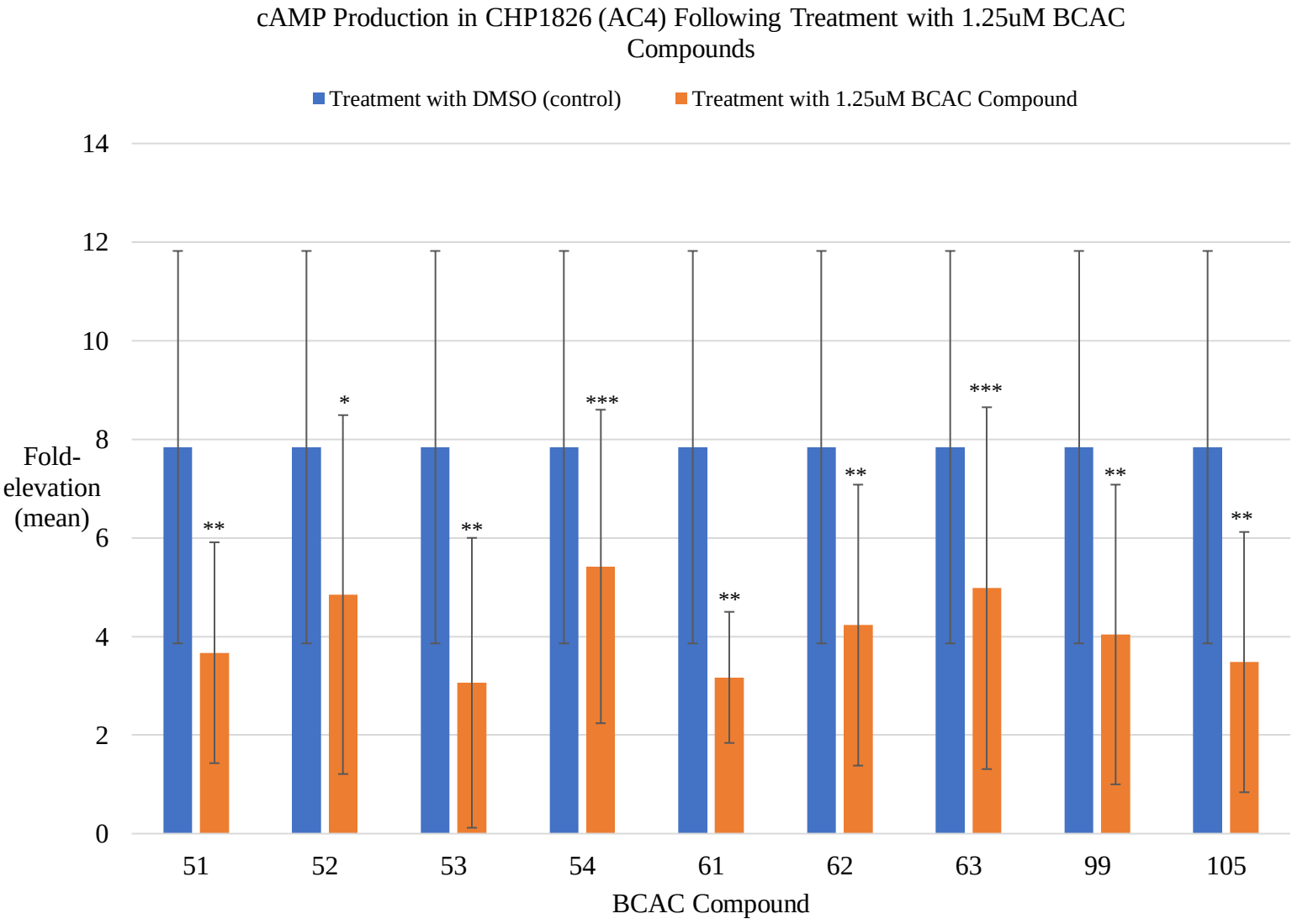

Figure 14. cAMP assays were conducted on CHP1963 (AC6). Cultures were treated with 1.25μM BCAC compound and DMSO vehicle controls (plus 40μM Rolipram), and they were incubated for 30 minutes following inoculation. Fold-elevation of cAMP was calculated as described beneath Table 8. The mean fold-elevation is graphed, and the standard deviation is represented by the error bars. Statistical significance was calculated as described beneath Table 8 and is indicated as follows: *=p<.10, **=p<.05, ***=p<.01.

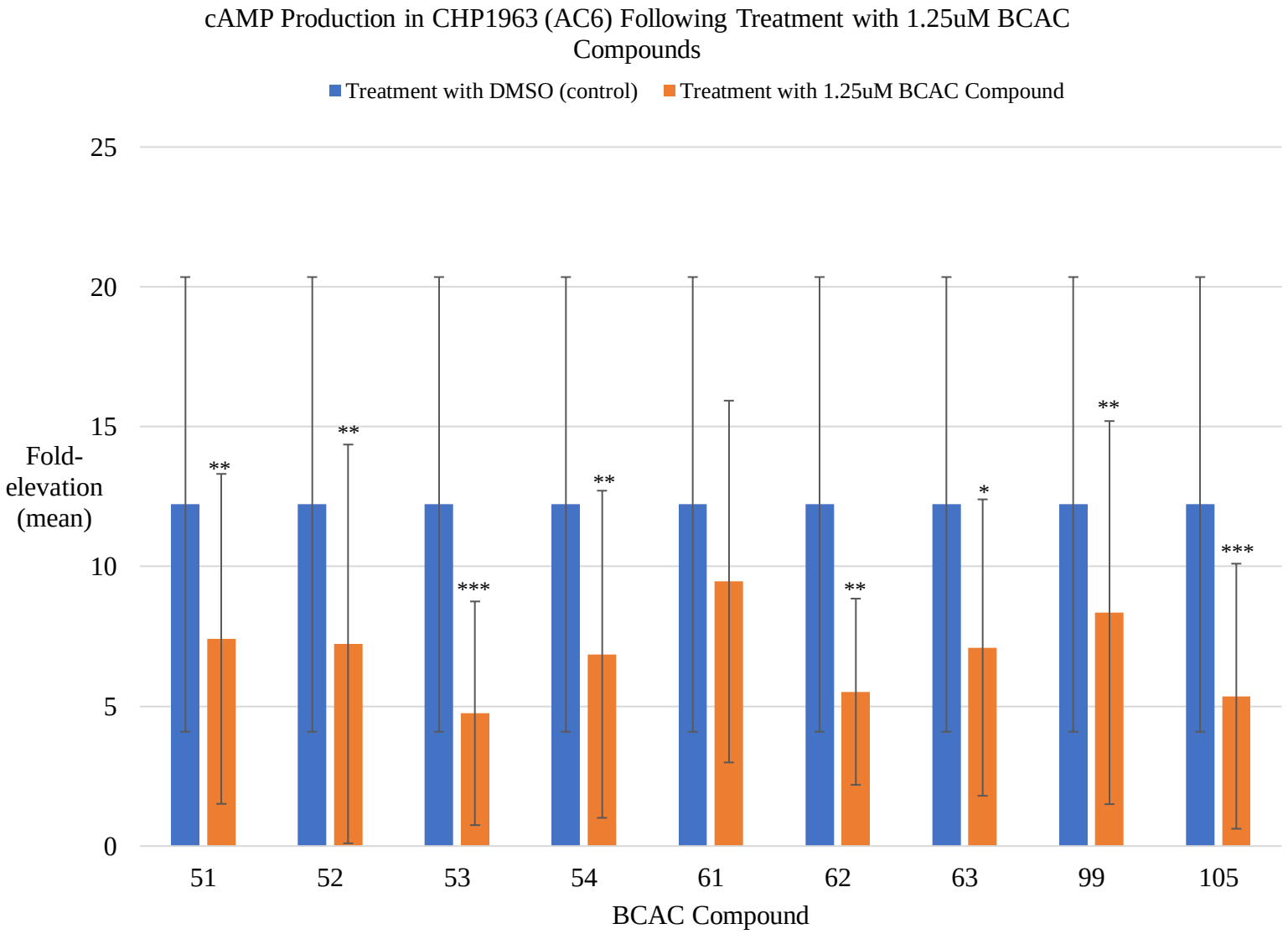

Figure 15. cAMP assays were conducted on CHP2027 (AC9). Cultures were treated with 1.25μM BCAC compound and DMSO vehicle controls (plus 40μM Rolipram), and they were incubated for 30 minutes following inoculation. Fold-elevation of cAMP was calculated as described beneath Table 8. The mean fold-elevation is graphed, and the standard deviation is represented by the error bars. Statistical significance was calculated as described beneath Table 8 and is indicated as follows: *=p<.10, **=p<.05, ***=p<.01.

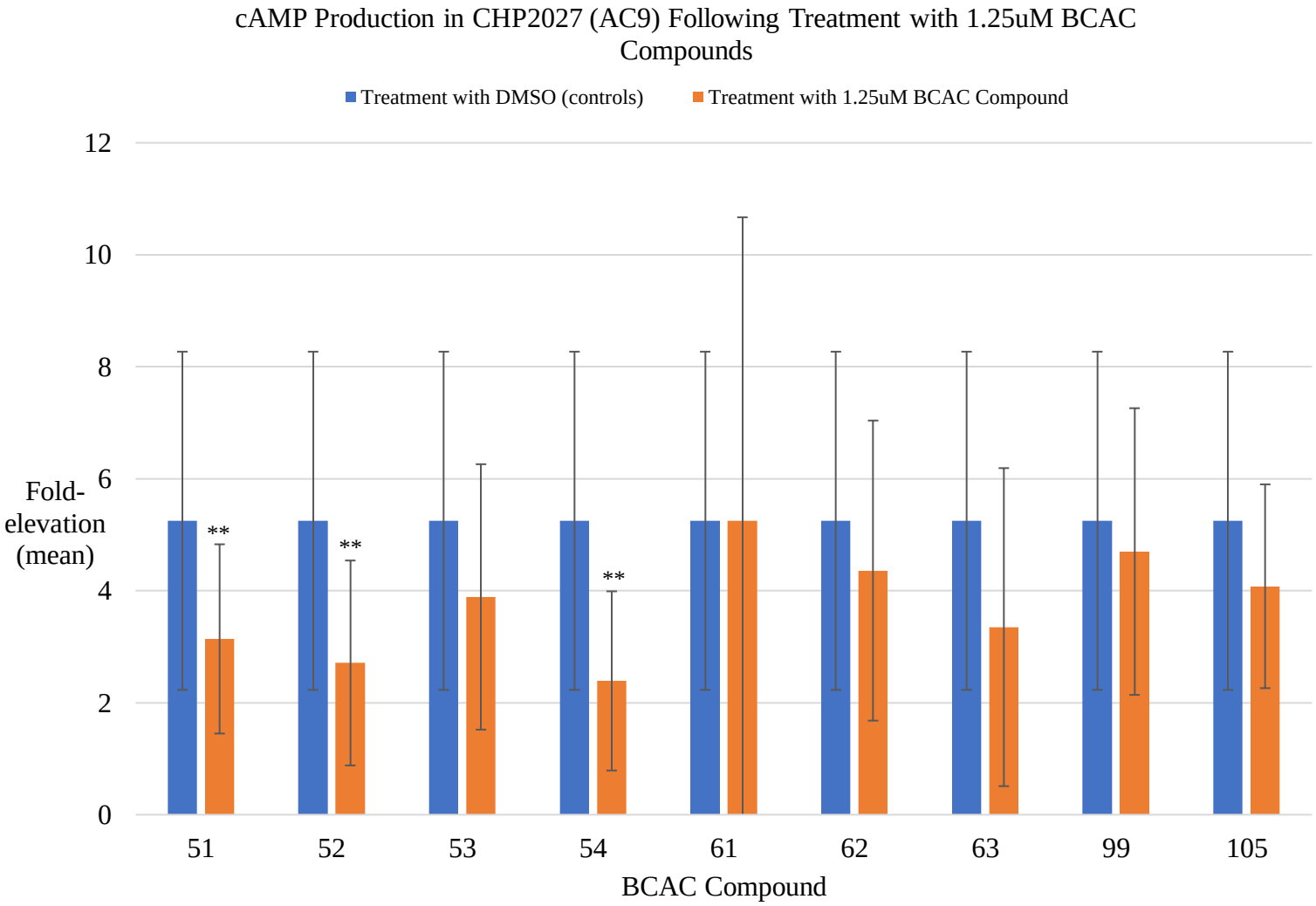

3.3 Interpretation and Discussion

These experiments were carried out to look for patterns of inhibition that might suggest whether the compounds directly act on the various ACs or act indirectly on something that regulates AC activity. If the BCAC compounds were to indirectly affect AC activity by binding to a target that is part of a pathway modulating AC activity downstream (such as calmodulin signaling or protein kinase C (PKC) phosphorylation), then the effects of compounds on different ACs would be expected to follow a pattern that reflects the potency of the compound on the target, combined with the importance of the target in regulating the activity of specific ACs. Since the compounds are structurally similar, it is reasonable to assume that they act on the same indirect target if they were to act on a pathway. Therefore, the differences in cAMP fold-elevation observed on each AC would be explained by the given AC's unique sensitivity to the impairment of the compound's target. However, the effects would likely vary slightly as a function of the compound's affinity for its target and of the state of the peripheral membrane environment of the AC (Dessauer *et al.* 2017).

If the compounds were to act by directly binding to and inhibiting the ACs, then one might expect to observe "cross-potency" wherein given compounds have significantly different effects on the cAMP fold-elevations of different ACs, as the schematic shows (Figure 16). This difference would be conferred by non-identical binding sites of the ACs, despite the high degree of conservation among the AC catalytic core (Zhang *et al.* 1997).

Figure 16. A schematic of cross-potency that is expected to reflect direct binding of BCAC compounds to ACs. In this hypothetical example, one compound (BCAC1) is significantly more effective inhibiting a particular AC (ACx) than is a second BCAC compound (BCAC2) (strength as an inhibitor corresponds to thickness of the arrows). The opposite trend might be observed for another AC (ACy), on which BCAC2 is significantly more effective than BCAC1.

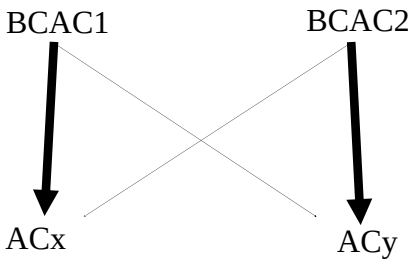

No statistically significant differences, as calculated by fold-elevation ratio (Table 8), were found among the compounds in terms of their ability to impact the ACs at all compound concentrations examined. Perhaps, one reason that statistical significance was not observed is that the compounds' binding sites on the ACs are highly conserved and that the differences in sensitivity are too small to be captured with the number of assays conducted. Other reasons may include the fact that the fold-elevation for the DMSO controls in some experiments was too low or that some compounds were not good enough inhibitors.

Interestingly, many BCAC compounds appeared to be less effective on AC5 and AC6 than on the other ACs at 2.5μM and 1.25μM. This may be due to the fact that AC5 and AC6 are both part of the same AC classification group (Group 3) and may have less conserved binding sites for

these compounds or, should these compounds actually work indirectly to affect AC activity, that these ACs are more resistant to inhibition of said activity.

BCAC54, 61, 62, 63, 66, and 67 were the most effective at reducing cAMP production to a statistically significant level (compared to DMSO vehicle controls) at all concentrations and across all ACs. The ACs examined are not calmodulin-sensitive (unlike Group 1 members AC1, 3, and 8), which suggests that the compounds do not act via interference with calcium calmodulin signal transduction (Dessauer *et al.* 2017). Some of the compounds show promise for future drug development. An analysis of Absorption, Distribution, Metabolism, and Excretion (ADME) on several compounds of the BCAC51 scaffold obtained their half-life, metabolism, and solubility data (James Inglese, pers. comm.). The results from BCAC63, 64, and 65 are the most favorable for potential passage to a further stage of investigation or modification for clinical use. BCAC63 is particularly enticing, as it was a highly potent inhibitor in the cAMP assays I conducted. Future work should include more cAMP assays on BCAC54, 61, 62, 63, 66, and 67 against various ACs in order to potentially observe statistically significant cross-potency effects that will better characterize the structure-activity relationships (SAR) and mechanism of action of these compounds.

The cAMP assays presented in this chapter were conducted in the presence of GNAS-stimulation. Therefore, the prospect that the compounds act by interfering with the G protein or with the GNAS-AC catalytic complex was not addressed by these data. A presentation and discussion of experiments involving AC in the absence of GNAS is reserved for Chapter 6.

4 ANALYSIS OF THE HUMAN WILD-TYPE AC5 GENE AND THE UNUSUAL R418W MUTANT ALLELE

4.1 Cloning and Sequencing of Wild-Type and Mutant Alleles of Human AC5

The human AC5 R418W mutation has been shown to confer increased sensitivity to GNAS (Dessauer *et al*. 2017). We therefore questioned whether this mutation affected GNAS-stimulated AC activity in response to the putative BCAC inhibitor compounds. The wild-type (wtAC5) and R418W mutant (mtAC5) alleles (courtesy of Val Watts) were amplified from mammalian expression vectors and cloned by gap-repair transformation into the pJV1 expression vector (Figure 17) (Kelly and Hoffman 2002, Bailey *et al.* 1986). PCR was used to confirm the presence of the gene. Plasmids were rescued to *E. coli*, and sequencing confirmed that each plasmid carried either wtAC5 or mtAC5.

Figure 17. This schematic shows the construction of pJV1 expression vectors carrying the *tif471* promoter and expressing either wtAC5 or mtAC5. Gap-repair transformation of each allele from mammalian expression vectors into pJV1 plasmids, which were digested with the restriction enzyme *Sac*II, was performed. pJV1 carried the *lys2* selectable marker, and transformants were selected for Lys$^+$.

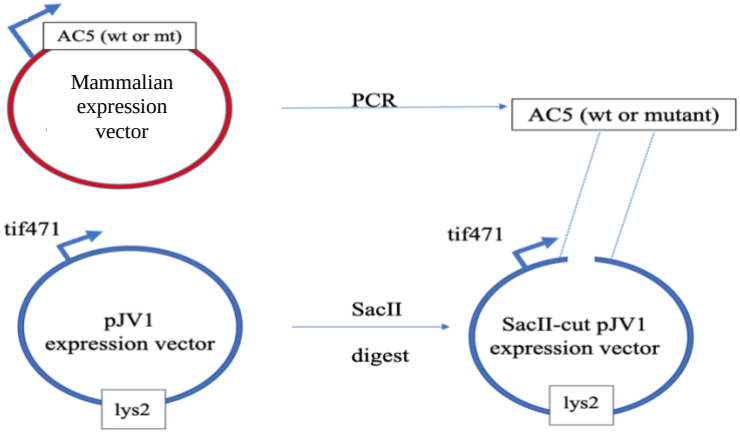

pJV1 vectors were transformed and integrated into strain CHP1831. Mitotically stable integration events with single-copy plasmids were indicated by colonies with a Lys$^+$ phenotype: plasmids were digested with *Nde*I, which cuts within the *lys2* gene to target recombination at the host *lys2* locus. To select for stable integrants, transformants were replica-plated from EMM-lysine to YES (nonselective) to allow cells carrying autonomously-replicating plasmids to lose the plasmid and revert to Lys$^-$, while cells in a colony carrying an integrated plasmid all remained Lys$^+$. After several rounds of replica plating to YES, colonies were replica plated back to EMM-lysine to check for stable Lys$^+$ colonies, which were regrowing more quickly than colonies with only a small number of Lys$^+$ cells. A representative example of the isolation of stable integrants is a wild-type colony growing well on EMM-lysine (Figure 18). To verify

integration of the plasmids, candidate strains CHP2445 and CHP2443 were crossed with CHP1466, and the progeny were examined for a 2:2 segregation of the *lys2*$^{+}$ selectable marker. This cross also served to exchange the *fbp1:GFP* reporter with *fbp1:ura4.*

Figure 18. A representative example of selecting colonies on EMM-lysine with mitotically stable, integrated plasmids. The example shown is of a wild-type AC5-carrying plasmid, which was transformed into CHP1831 and selected for on EMM-lysine. Colonies were replicated onto EMM, to result in loss of autonomously-replicating plasmids. Colonies were replicated back to EMM-lysine to select for well-growing Lys^{+} colonies, such as the one circled on this EMM-lysine plate.

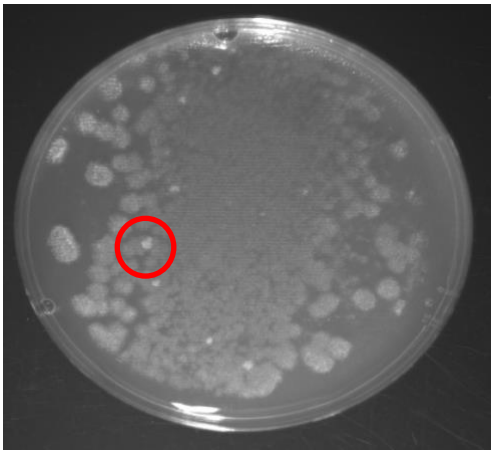

4.2 Wild-Type and Mutant AC5 Show Similar Sensitivity to Most BCAC Compounds

Strains expressing the wild-type human AC5 gene (CHP2445) and the AC5 gene carrying the R418W mutation (CHP2443) were analyzed through cAMP assays in the presence of BCAC compounds, to assess whether the mutant and wild-type AC5 varied in their sensitivity to the compounds. Both CHP2445 and CHP2443 also expressed mutationally-activated GNAS

($GNAS^{R201C}$) such that the ACs were stimulated. Experiments were carried out with a 30-minute incubation period following treatment of the culture with 5μM compounds and 40μM Rolipram (to inhibit the mammalian PDE4D2 phosphodiesterase in these strains, thus triggering an increase in cAMP levels to reflect AC activity). Some experiments carried out earlier on did not include the later-adopted step of incubating cells in acetonitrile for 15 minutes at room temperature prior to centrifugation, thus potentially reducing the amount of cAMP extracted. cAMP production was calculated as a fold-elevation over time for both DMSO vehicle controls and compound-treated samples, and the results were compared to determine statistical significance (paired t-test, two-tailed). The data for each strain is shown (Tables 14-15, Figure 19). The fold-elevations of the controls ranged over the compounds tested on each allele, and cAMP production in the controls was sometimes greater than that in the compound-treated samples. This is most likely due to quality of the growth medium or to cells' varying responses to Rolipram. The results of some experiments did not show at least a 3-fold elevation of cAMP in the DMSO-treated control or showed the "time=0 minutes" read as having the highest amount of cAMP, likely reflecting an issue with the cultures. Therefore, these results were not included in the calculations, and this resulted in the elimination of no more than 2 experiments for each strain.

Table 14. cAMP Production in CHP2445 (wtAC5) Following Treatment with BCAC Compounds

BCAC Compound of Treatment (5μM)	Fold-elevation – DMSO controls (mean)	Fold-elevation – DMSO controls (std. dev.)	Fold-elevation – BCAC compound (mean)	Fold-elevation – BCAC compound (std. dev.)	Number of assays
51	15.25	10.64	13.72	12.48	3
54	12.47	6.02	7.53**	4.09	11
61	12.47	6.02	3.81***	1.36	11
62	14.26	8.06	5.72***	3.13	26
63	12.47	6.02	5.20***	2.43	11
66	12.47	6.02	6.50***	2.86	11
67	12.47	6.02	6.95***	3.41	11
70	5.78	2.22	5.3	0.92	4
87	5.78	2.22	5.13	1.75	4
88	5.78	2.22	6.72	1.57	4
89	5.78	2.22	6.53	1.69	4
90	5.78	2.22	3.65	1.19	4
91	5.78	2.22	6.3	1.75	4
92	6.1	2.05	6.77	1.84	5

Statistical significance was calculated as described beneath Table 8 is indicated as follows (paired t-test, two-tailed):

*=p<.10, **=p<.05, ***=p<.01. cAMP production was calculated as a "fold-elevation," according to the following ratio:

$$elevation = \frac{\text{extracted cAMP (units: spectral counts) at T=30 minutes after compound treatment}}{\text{extracted cAMP (units: spectral counts) at time of compound treatment (T=0 minutes)}}.$$

Table 15. cAMP Production in CHP2443 (mtAC5) Following Treatment with BCAC Compounds

BCAC Compound of Treatment (5μM)	Fold-elevation – DMSO controls (mean)	Fold-elevation – DMSO controls (std. dev.)	Fold-elevation – BCAC compound (mean)	Fold-elevation – BCAC compound (std. dev.)	Number of assays
51	11.13	1.75	10.77	5.46	3
54	12.39	7.14	7.86***	5.02	11
61	12.39	7.14	4.84***	1.75	11
62	14.51	9.82	9.14***	5.25	26
63	12.39	7.14	6.54***	3.56	11
66	12.39	7.14	8.13**	4.74	11
67	12.39	7.14	7.95**	5.18	11
92	21.26	11.69	28.32	7.12	2

Statistical significance was calculated as described beneath Table 8 and is indicated as follows: *=p<.10, **=p<.05, ***=p<.01. Fold-elevation of cAMP was calculated as described beneath Table 14.

Figure 19. cAMP elevation in strains carrying (A) AC5 wild-type (CHP2445, wtAC5) and (B) mutant (CHP2443, mtAC5) alleles was analyzed over a 30-minute period following treatment with 5μM inhibitor compounds, plus 40μM Rolipram, and measured by mass spectrometry. The fold-elevation was calculated as described beneath Table 14. Statistical significance was calculated as described beneath Table 8 is indicated as follows: *=p<.10, **=p<.05, ***=p<.01.

(A)

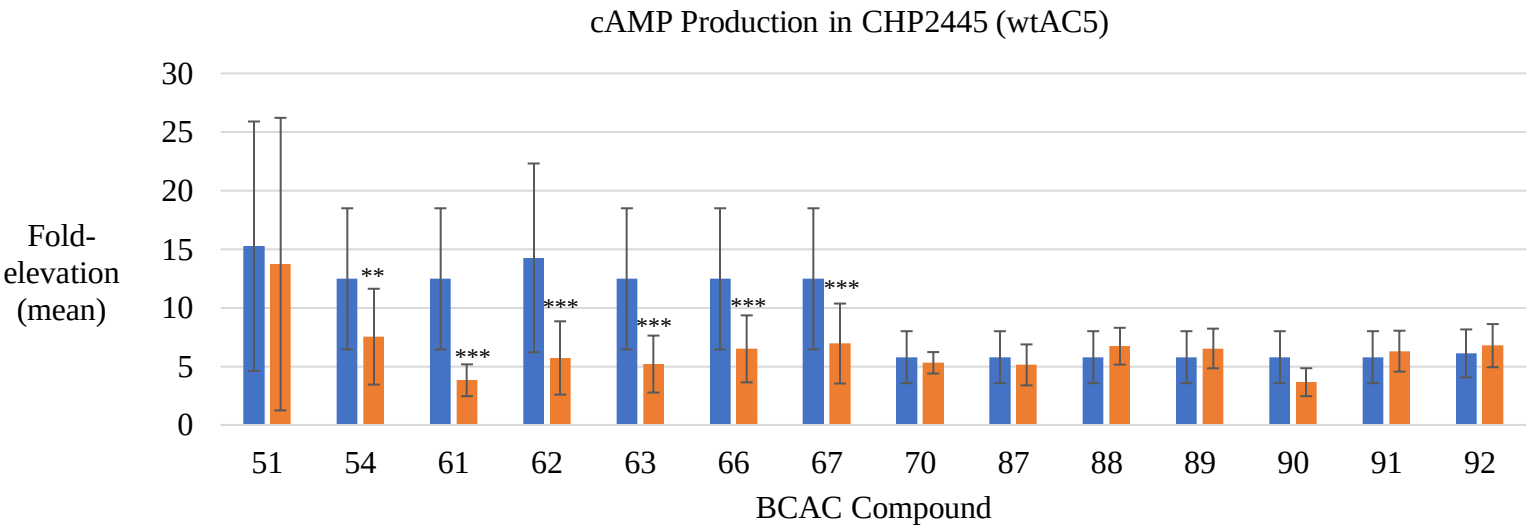

(B)

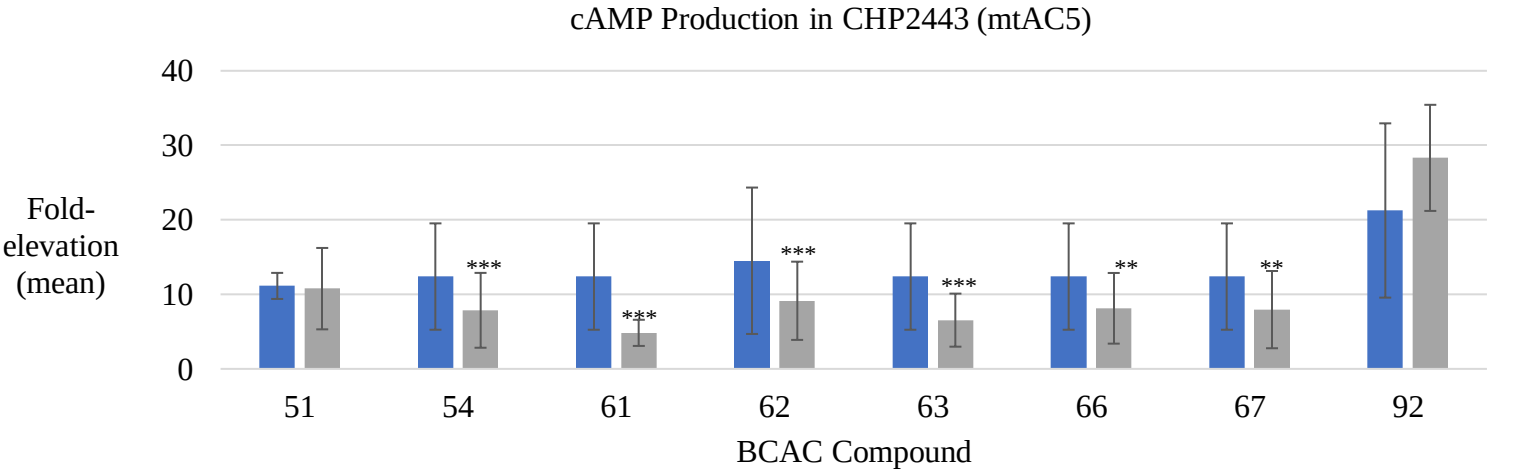

4.3 Interpretation and Discussion

Human AC5 alleles containing the R418W mutation have been shown to confer an increased sensitivity to GNAS. Several disease states have been linked to the R418W mutation, including familial dyskinesia, chorea, and dystonia (Chang *et al.* 2016). Therefore, it was of interest whether any BCAC compounds were more potent on mtAC5 than on the wild-type allele, as they would likely be favorable for potential development into drugs.

In the analysis, the wild-type and mutant alleles appeared to respond to BCAC compounds with similar significance. However, as measured by fold-elevation ratio (Table 8), wtAC5 appeared to respond much more sensitively to BCAC62 (mean ratio=0.40) than did mtAC5 (mean ratio=0.75) ($p<.10$). However, the mechanism (direct or indirect action of the compound) behind this difference is unclear. The trend discussed in Chapter 3 that AC5 appears to be less sensitive than the other ACs holds true according to the 5μM analysis. AC5 is part of a different AC classification group than the other ACs, which could explain this result (Dessauer *et al.* 2017).

5 SENSITIVITY OF ACs TO BCAC COMPOUNDS IN THE ABSENCE OF GNAS-STIMULATION

5.1 cAMP Assays Fail to Measure Compound Sensitivity of Basal-ACs

At first, cAMP assays, as described in Chapters 3 and 4, were conducted with strains expressing various ACs but not GNAS (basal-ACs), since these assays were previously successful in addressing whether the compounds affect AC activity in the presence of GNAS. However, a very low signal was being read off the mass spectrometer which reflected the low level of cAMP production expected in the absence of GNAS-stimulation. Therefore, it was impossible to determine whether the compounds affected basal-AC activity, and the decision was made to pivot to a potentially more sensitive technique.

cAMP increases PKA activity, which can be monitored by expression of the *fbp1:GFP* reporter. GFP fluorescence is expected to inversely correspond to AC activity. I therefore examined the possibility of assessing basal-AC activity by GFP flow cytometry, which would separate cells based on their fluorescence signal.

5.2 Assessing Basal-AC Activity Via GFP Flow Cytometry

Twenty-three strains, carrying a variety of combinations of AC in the absence of GNAS (either AC1, AC2, AC4, AC5, AC6, AC7, or AC9) together with various PDEs, were profiled to determine their baseline fluorescence signal prior to any treatment with inhibitor compound. Control strains carrying no mammalian AC, which would respond to compounds through induction of *fbp1* via MAPK-mediated stress response, were also analyzed. Ultimately, five

strains were selected for further study as they displayed an intermediate level of fluorescence signal near the Quadrant 3/Quadrant 4 (Q3/Q4) border (Q3=low fluorescence and Q4=high fluorescence) (Figure 20). As such, these strains might have been the most likely to display a response to compound treatment. In addition to showing the distribution of cells displaying varying levels of fluorescence, a median fluorescent intensity (MFI) of the population provides a value that can be used as a quantitative measure of the culture. These strains express four different mammalian ACs, along with one control strain that expresses the *S. pombe* Git2 AC.

Figure 20. Flow cytometry readouts for (A) a low-GFP, negative control strain (CHP731) and (B) a high-GFP, positive control strain (CHP2486) used during experiments with basal-AC strains are shown. (C) A representative flow cytometry readout for basal-AC strains exhibiting the "intermediate-GFP-fluorescent" phenotype, which were those exhibiting a range of fluorescence signal near the Q3/Q4 border, is shown for CHP1925 (AC7). (D) A representative flow cytometry readout for strains exhibiting the "high-GFP-fluorescent" phenotype, which were those exhibiting a range of GFP signal almost entirely in Q4, is shown for CHP1822 (AC5). The percentage of cells in Q3 and Q4, relative to the total amount in each sample, is nested in each respective quadrant. GFP signal was measured by median fluorescent intensity (MFI).

(A)

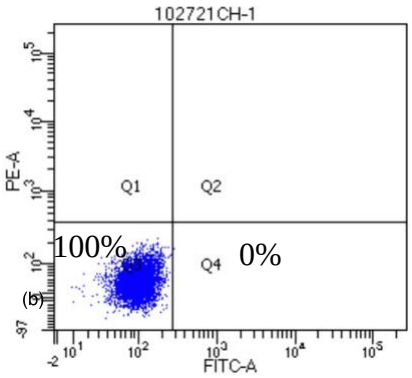

MFI = 100

(B)

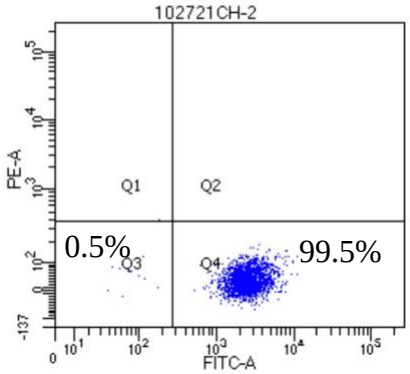

MFI = 2456

(C)

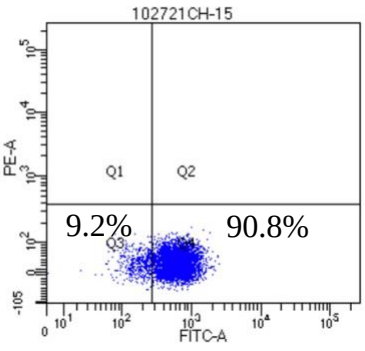

MFI = 596

(D)

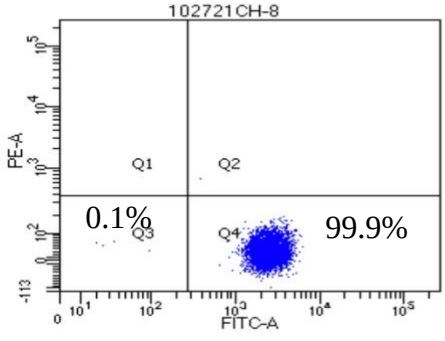

MFI = 2416

5.3 Selection of BCAC61 and BCAC63 as Test Compounds

To determine what compound(s) to use in the flow cytometry experiments, I initially examined the effect of nine compounds on CHP1919 (AC4) by GFP fluorescence. Since AC4 had been distinguished by its high degree of sensitivity to inhibitor compounds in earlier experiments (see Chapter 3), CHP1919 was selected for this analysis. The fluorescence of cells following overnight treatment with nine compounds, selected because of their effectiveness in reducing cAMP levels during previously conducted assays, was examined (Figure 21). Treatment with 2μM compounds was selected because it was not so high a concentration as to affect cell growth but was enough to observe a GFP response.

Figure 21. Strain CHP1919 (AC4) was subjected to fluorescence microscopy following treatment with 2μM of a variety of BCAC compounds plus DMSO (vehicle control). Cultures were inoculated and grown overnight, and they were visualized using the EVOS with a 4X objective.

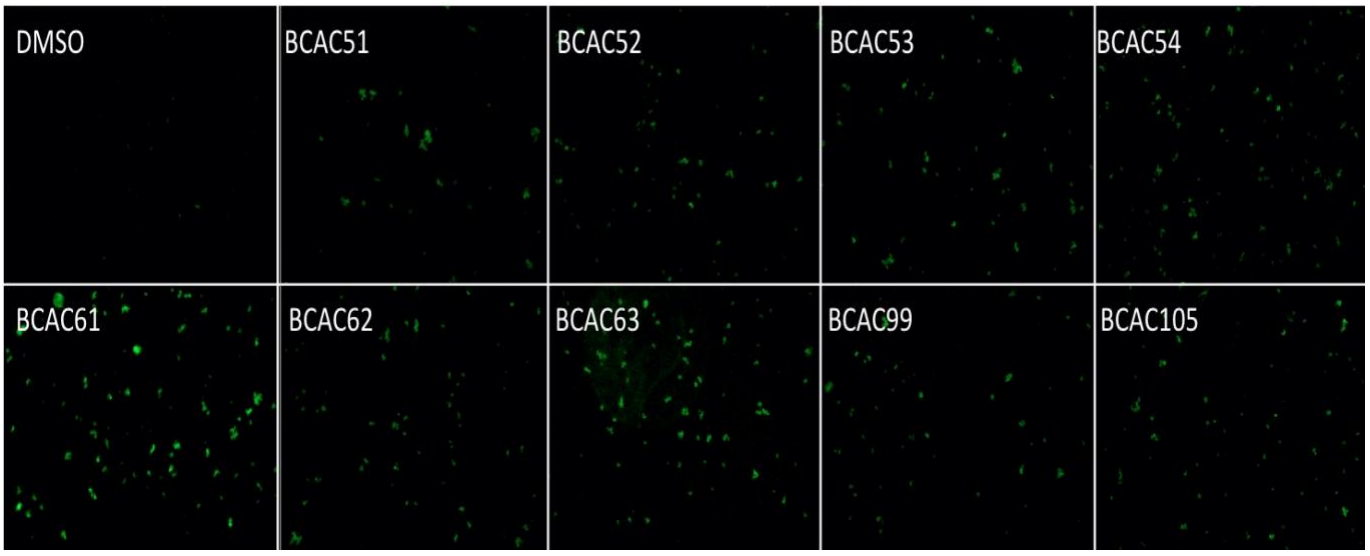

The highest level of fluorescence was observed following treatment with BCAC61 and BCAC63, suggesting that these compounds were the most effective at derepressing the *fbp1:GFP* reporter and, therefore, potentially the most potent inhibitors of AC4. Next, a culture of strain CHP1919 was examined following treatment with DMSO, BCAC61, or BCAC63 using differential interference contrast (DIC) light microscopy to analyze cell morphology, as well as fluorescence microscopy and flow cytometry to examine GFP signal (Figure 22). The morphological changes (shortening of cell length and rounding of cells) as well as the increase in GFP fluorescence were observed upon treatment with these compounds. This is consistent with the conversion of cells to a low-PKA phenotype. Furthermore, the alignment of flow cytometry and microscopy data suggested that flow cytometry experiments would be suitable for analysis of these basal-AC strains.

Figure 22. One culture of strain CHP1919 (AC4) was analyzed following treatment with either DMSO, 2μM BCAC61, or 2μM BCAC63. Cultures were grown overnight. Two phenotypes were examined: (A) cell morphology using differential interference contrast (DIC) light microscopy, (B) GFP signal using fluorescence microscopy, and (C) flow cytometry. Microscopy was conducted using a 40X objective on the Zeiss.

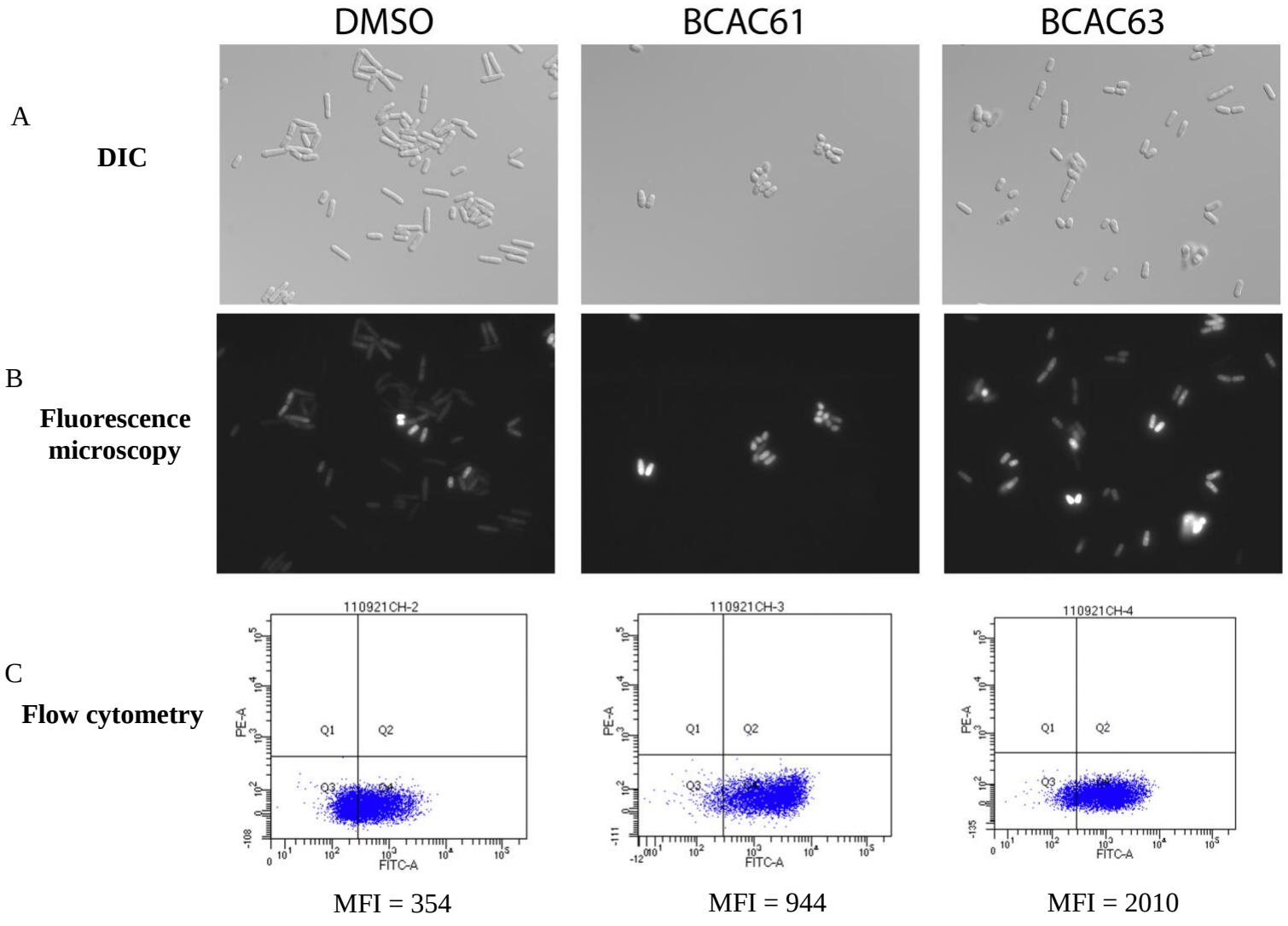

5.4 Profiling Basal-ACs Following Treatment with BCAC Compounds

Flow cytometry assays on the four selected mammalian AC-expressing strains plus CHP1744 were conducted to examine the effect of the compounds on basal-AC activity. A representative flow cytometry readout for an experiment of treatment with either DMSO, 2μM BCAC61, or 2μM BCAC63 is shown for each strain (Figure 23). Average GFP fluorescence signal (median fluorescent intensity) is also shown for these experiments (Figure 24, Table 16). A statistically significant increase in GFP signal was observed upon treatment with both BCAC61 and BCAC63 for strains expressing AC2 and AC4 ($p<.01$) and upon treatment with BCAC61 for a strain expressing AC9 ($p<.05$). Treatment of the AC7-expressing strain with either compound or of the AC9-expressing strain with BCAC63 led to a large elevation of the MFI, however these did not reach statistical significance. In contrast, the average MFI of cultures of the Git2-expressing strain was actually lower in the compound-treated cultures than in the DMSO-treated cultures.

Figure 23. Representative flow cytometry readouts for GFP assays of four mammalian AC-expressing strains and *S. pombe* Git2 AC-expressing CHP1744. GFP signal was evaluated by median fluorescent intensity (MFI). Samples were inoculated with either DMSO, 2μM BCAC61, or 2μM BCAC63 and incubated overnight.

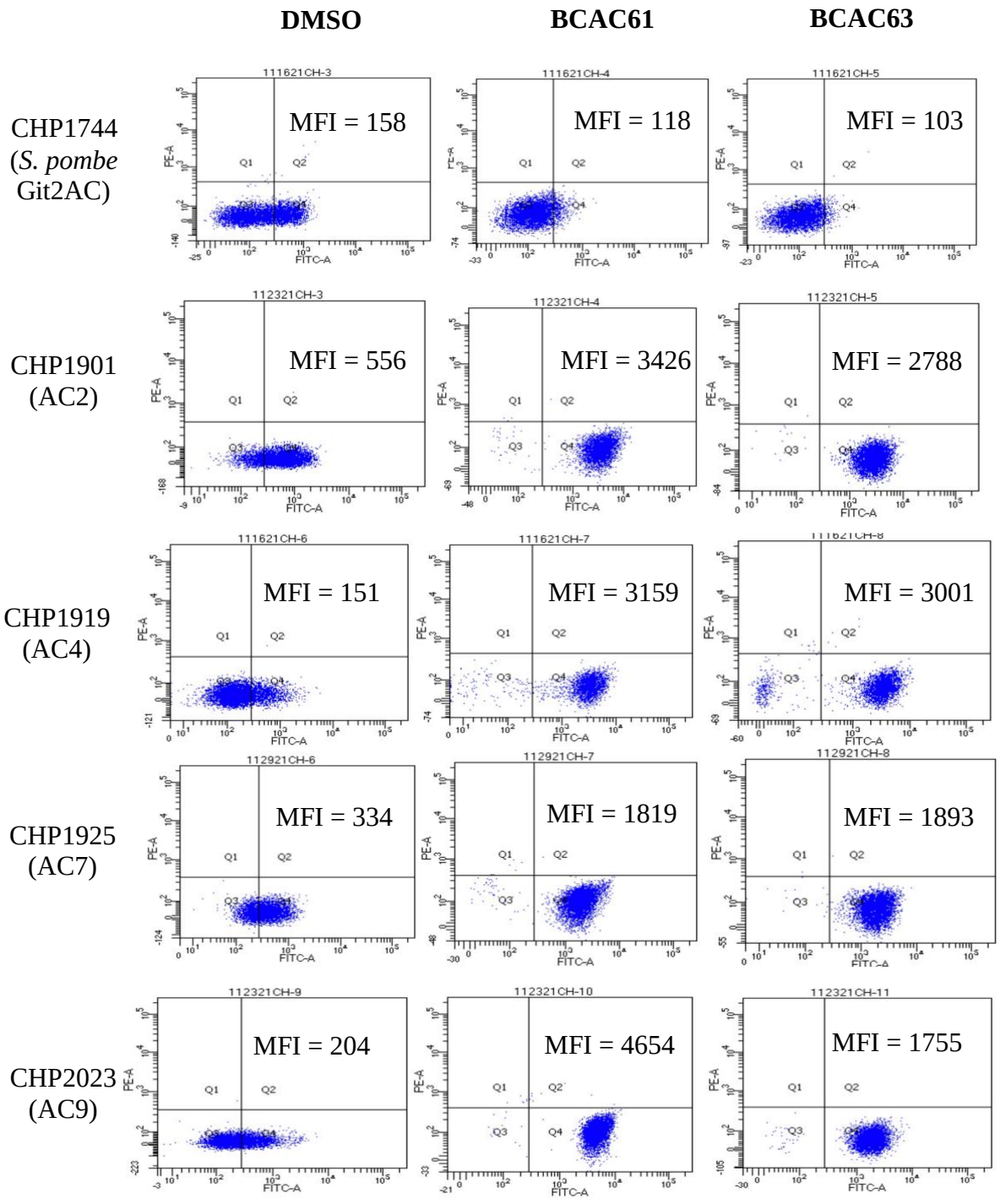

Table 16. Average of Median Fluorescent Intensity (MFI) Across Flow Cytometry Experiments Involving Treatment with 2μM BCAC61 and 2μM BCAC63

Strain (AC)	MFI (DMSO control) (mean)	MFI (DMSO control) (SD)	MFI (BCAC61) (mean)	MFI (BCAC61) (SD)	MFI (BCAC63) (mean)	MFI (BCAC63) (SD)
CHP1744 (Git2AC)	324.67	215.48	201.67	72.84	170.33	61.33
CHP1901 (AC2)	955.5	564.98	3823***	561.44	3216***	605.28
CHP1919 (AC4)	571.67	541.38	2918.67***	822.42	3326***	2087.24
CHP1925 (AC7)	297	52.33	1212.5	857.72	1367	743.88
CHP2023 (AC9)	766.5	795.5	4972**	449.72	3560	2552.66

Statistical significance is indicated as follows and is the result of a paired t-test (two-tailed) that compared MFI values of each strain's samples treated with DMSO with those treated with BCAC61 or BCAC63: *=p<.10, **=p<.05, ***=p<.01.

Figure 24. The average of the median fluorescent intensities (MFIs) from the flow cytometry experiments conducted on four basal-AC-carrying strains and one *S. pombe* Git2 AC control strain (CHP1744) is graphed below. Samples were treated with either DMSO (vehicle control), 2μM BCAC61, or 2μM BCAC63. A paired t-test (two-tailed) was conducted for each strain that compared average fluorescent intensity for the DMSO vehicle control sample with the average fluorescence intensity for the compound-treated sample, and statistical significance is indicated above the respective strain's compound data according to the following legend: *=p<.10, **=p<.05, ***=p<.01.

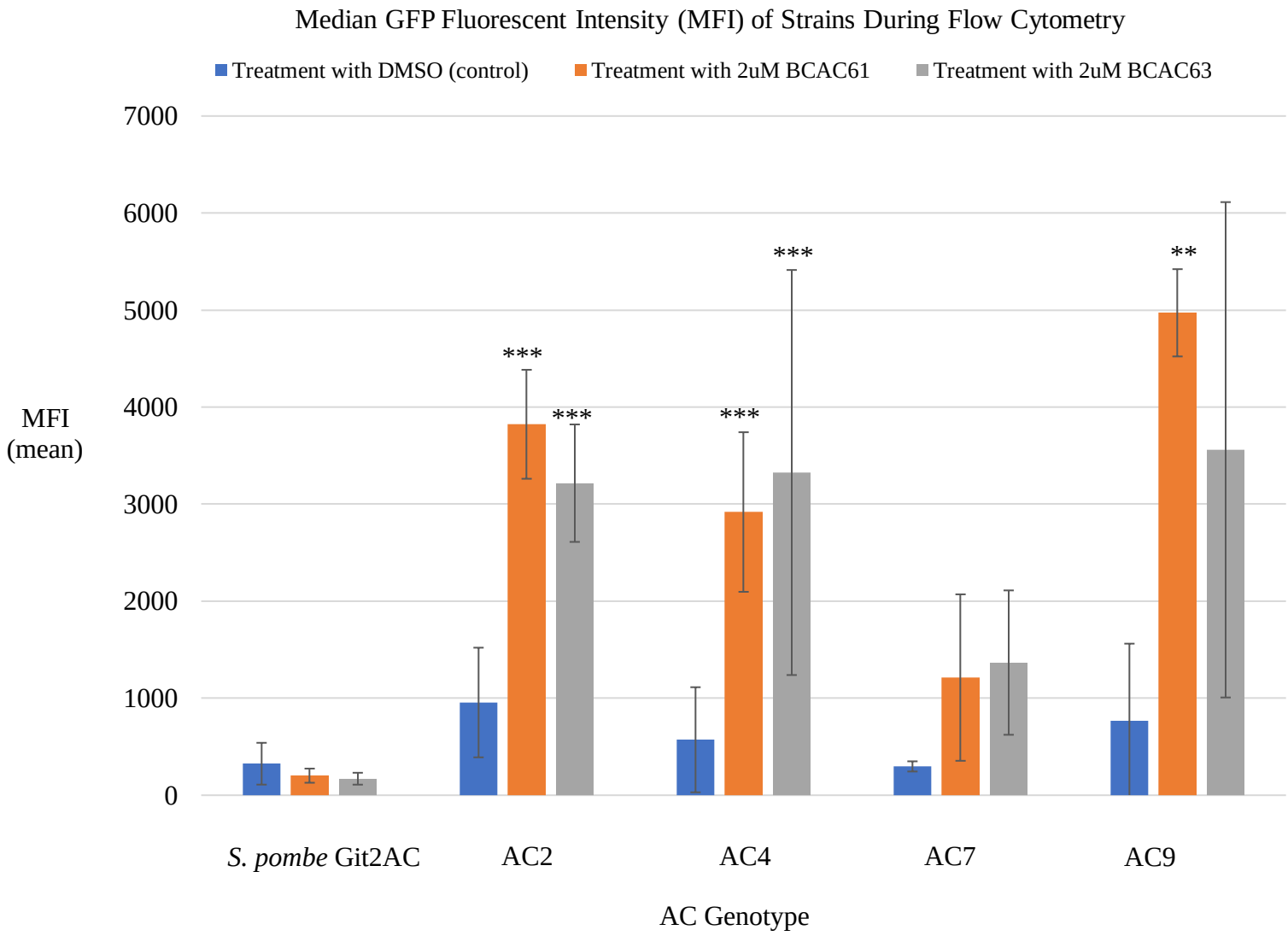

5.5 Interpretation and Discussion

Flow cytometry as a means of analyzing strains carrying mammalian ACs in the absence of GNAS was shown to be more feasible than cAMP assays, as the cAMP assays were too insensitive to the low level of cAMP production that occurred in the absence of GNAS. The negative, low-GFP (CHP731) and positive, high-GFP (CHP2486) control strains were important during the flow cytometry readouts in delineating the border between Q3 and Q4 that would be used in flow cytometry experiments.

BCAC61 and BCAC63 were determined to be effective at shifting the GFP signal from low to high upon strains expressing AC2, AC4, AC7, and AC9. The strains did not express AC-stimulating GNAS and, therefore, the effect of the compound on basal-AC activity was observed. The statistically significant increase in GFP signal, represented as median fluorescent intensity, on AC2, AC4, and AC9 rules out the possibility that BCAC compounds act by inhibiting GNAS directly or by interfering with the AC-GNAS stimulatory complex. Furthermore, as both CHP1901 (AC2) and CHP1744 (Git2) both express rat PDE4A5, the differential response to these compounds cannot be explained by PDE stimulation to lower cAMP levels. Thus, while these results do not require the BCAC compounds to act directly on the ACs, they do rule out several other mechanisms by which they could lower cAMP levels as seen in Chapter 3.

6 DESIGNING AND CONDUCTING A MOLECULAR GENETIC SCREEN TO DETECT COMPOUND-RESISTANT AC MUTANT ALLELES

A molecular genetic screen for AC mutations conferring compound-resistance was developed and piloted using flow cytometry in an effort to find mutations in an AC gene that might reveal the site of action of the BCAC compounds. In this, a population of mutated plasmids were screened for ones that produce an AC that remains active in the presence of an inhibitor compound as judged by a low GFP signal (high PKA activity). The development of this assay required the selection of a strain expressing a PDE whose activity would be overwhelmed by the cAMP production due to a plasmid-expressed AC, as well as a BCAC compound that would shift the balance of AC versus PDE activity to produce a low-PKA, high-GFP signal.

6.1 Selecting a Compound and Compound Concentration

Growth-inhibition assays were done on strains expressing AC4, AC5, and AC7, which consisted of treating cultures with all 41 members of the BCAC51 scaffold of compounds at 2.5μM and 1.25μM. GFP signal was assessed to represent PKA activity, which was expected to correspond with the degree of AC inhibition. In addition, optical density was inversely measured as a proxy for growth inhibition, a phenotype associated with high concentrations of many BCAC compounds. BCAC61 and BCAC63 were found to confer a high-enough GFP signal, such that a low-to-high shift in fluorescence could be detected upon inoculation, without imparting significant growth inhibition (data not shown). Further profiling by flow cytometry on strains expressing AC4, AC5, AC6, and AC9 and inoculated with compound concentrations ranging from 0.5μM to 4μM revealed that inoculation with BCAC63 at 2.5μM produced the highest

increase in GFP signal upon inoculation. Therefore, BCAC63 at 2.5μM was chosen for the genetic screen.

6.2 Selecting a Target AC

The target AC to be used in the genetic screen was determined to be AC9 after a series of profiling experiments on various ACs. A strain expressing AC9 showed the largest low-to-high shift in GFP signal upon treatment with BCAC63. A representative flow cytometry readout following treatment with 2.5μM BCAC63, plus a DMSO vehicle control, is shown. (Figure 25).

Figure 25. A representative flow cytometry readout following treatment of CHP2027 (AC9) with 2.5μM BCAC63, plus DMSO as a control, is shown. Cells were cultured overnight. GFP signal was measured by median fluorescent intensity (MFI). The shift in GFP signal from MFI=61 to MFI=250 upon treatment with compound suggested that AC9 treated with 2.5μM BCAC63 would be a suitable setup for the genetic screen for compound-resistant mutant alleles.

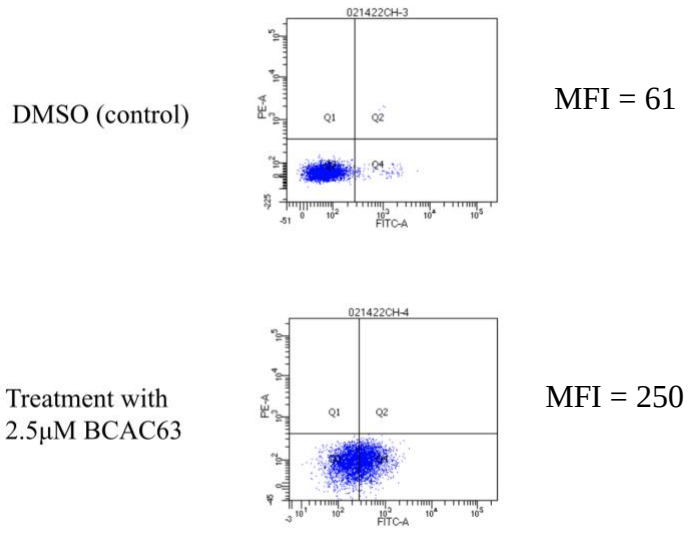

6.3 Generation of Mutant AC9 Alleles

XL-1 Red competent *E. coli* cells were used to generate mutations in the AC9 allele. XL-1 Red is a mutator strain that is deficient in three DNA repair mechanisms, so that the passage of a plasmid through it generates a collection of randomly mutated plasmids (Muteeb and Sen 2010). Two pools of pJV1-AC9 transformants were isolated, and one of these pools' DNA was used to transform *S. pombe* (CHP2489) to Lys^+.

6.4 Isolation of Low-GFP-Fluorescent Candidates

Transformants were grown overnight in the presence of 2.5μM BCAC63 before being subjected to fluorescent-activated cell sorting (FACS). Cells with a fluorescent signal of less than 50 were sorted and collected potentially expressing compound-resistant mutant AC9 alleles, as BCAC63 had been previously shown to shift almost all cells expressing wild-type AC9 to a higher value than 50 (Figure 26). Sorted cells were initially plated to form single colonies on YES plates before testing to see whether the plasmid was responsible for the low GFP signal.

Figure 26. Yeast transformants carrying plasmids, which carried mutational AC9 DNA prepared from XL-1 Red competent *E. coli* cells, were treated with 2.5μM BCAC63 and DMSO (vehicle control) and incubated overnight. Cells with MFI<50 were sorted and plated to YES. The cutoff of MFI=50 targeted cells at the "tail" of the GFP signal distribution of compound-treated cells for sorting.

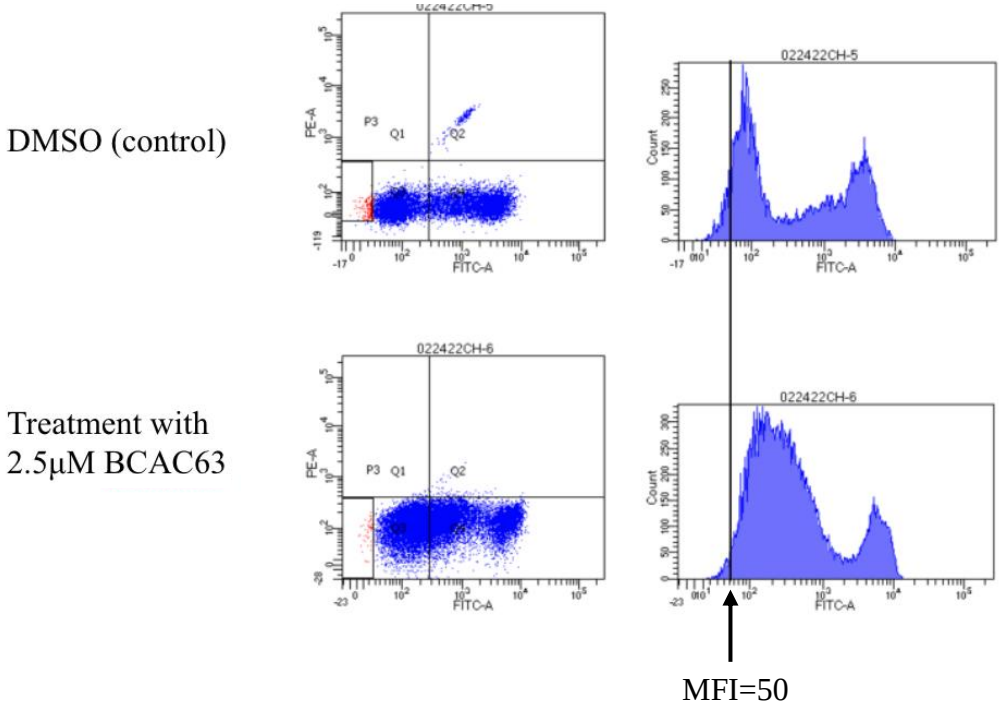

6.5 Examination of Plasmid Loss

The sorted cells were replica-plated from YES onto EMM-lysine and EMM-histidine plates. EMM-histidine would allow all cells to grow regardless of whether or not they carried the pJV1-AC9 plasmid. By comparing the GFP signal from cells in which the plasmid could be lost to that of cells growing on EMM-lysine that should retain the plasmid, one can determine whether the plasmid AC is responsible for the low GFP signal versus a host mutation. If the plasmid is responsible, there should be a higher GFP signal in the EMM-histdine-grown culture. If a host mutation is responsible, such as in the *cgs1* PKA regulatory subunit gene (Stiefel *et al.* 2004), the

GFP signal would remain low even after plasmid loss. The EMM-histidine and EMM-lysine replica plates were visualized by fluorescence microscopy, and candidate colonies that showed a high GFP signal on EMM-histidine and whose equivalent colonies on EMM-lysine showed a low GFP signal were selected for further analysis. Six candidates were selected. The equivalent candidates from both EMM-histidine and EMM-lysine were assessed by flow cytometry to test for plasmid loss, and two representative candidates are shown (Figure 27). Candidate 1 shows a clear elevation in the GFP signal upon plasmid loss, while the elevation in candidate 2 is more modest.

Figure 27. Candidate colonies carrying mutated AC9 alleles that exhibited high GFP in nonselective media (EMM-histidine) and low GFP signal in selective media (EMM-lysine) were read by flow cytometry to test for plasmid loss. Results from two representative candidates are shown.

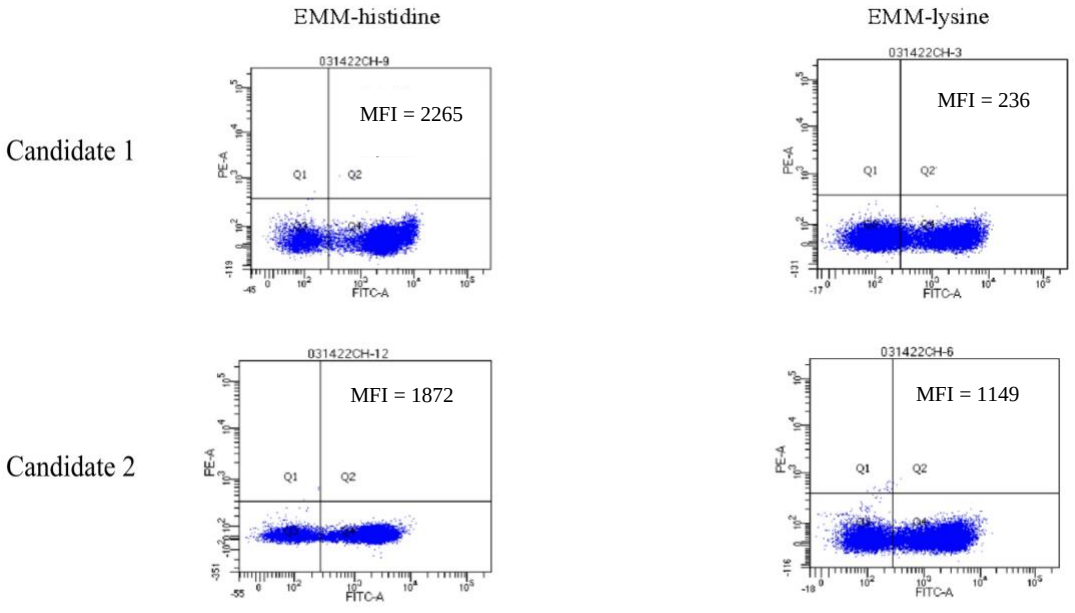

6.6 Testing Candidates for Non-Responsiveness

Flow cytometry was conducted on the candidates, which were treated with either DMSO or 2.5µM BCAC63 to test for non-responsiveness, which would potentially indicate a compound-resistant mutant. Cultures were incubated overnight. The results from the same two candidates shown in Figure 27 are shown (Figure 28).

Figure 28. Flow cytometry readouts are shown for experiments in which the two candidates were treated with either DMSO or 2.5µM BCAC63 and incubated overnight. Their non-responsiveness was examined in order to potentially determine the existence of a compound-resistant mutant allele.

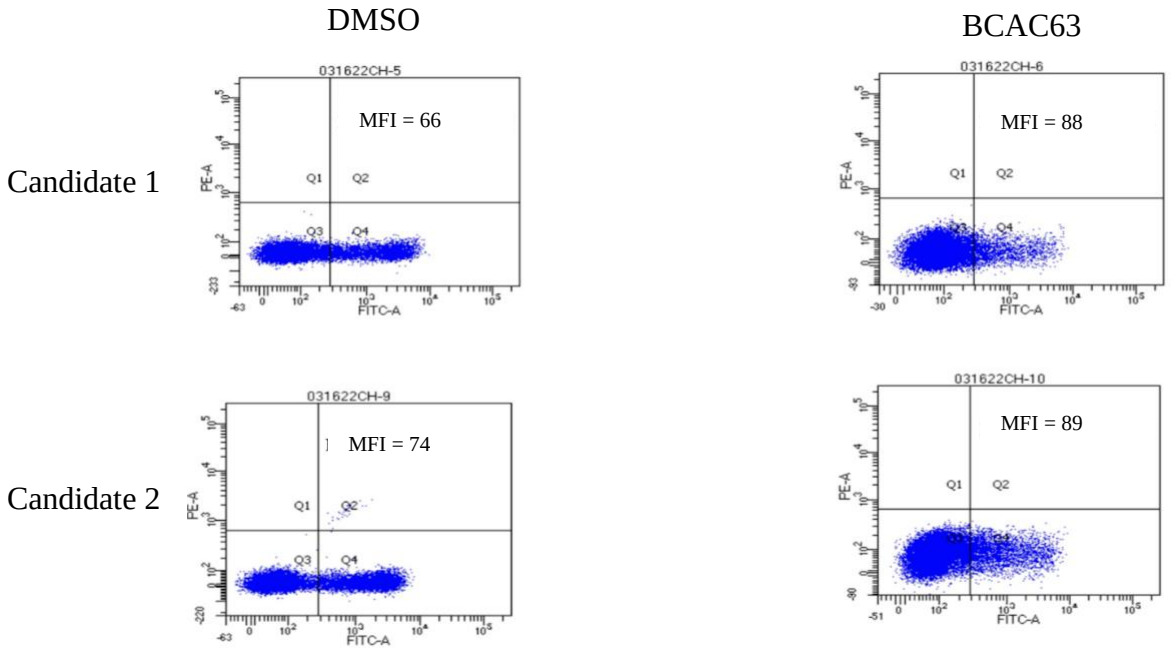

Plasmids were rescued from the candidates and used to transform ElectroTen-Blue competent *E. coli* cells for amplification. Plasmids were prepared from *E. coli* and used to transform yeast

(CHP2489). Another flow cytometry experiment to test for non-responsiveness was attempted to be performed, but a control strain transformed with pJV1-AC9 (wild-type) was also not showing a low-to-high shift in GFP. Therefore, we were unable to proceed with these candidates. Some preliminary experiments have suggested that inoculating cultures while at a cell density of 10^6 cells/mL is optimal, and future experiments should consider this and other parameters in undergoing the steps of this genetic screen (data not shown).

6.7 Interpretation and Discussion

This chapter describes the development of a plasmid-based molecular genetic screen for mutant alleles of a mammalian AC gene that produce an AC displaying some degree of resistance to inhibition by BCAC compounds. While a pool of pJV1-AC9 transformants showed a sufficient shift from a low to a high GFP signal that allowed for sorting of candidate mutant transformants, the full cycle of sorting and testing has not been completed as of now.

If the strain transformed with pJV1-AC9 were to show a low-to-high shift in GFP signal following treatment with 2.5μM BCAC63, then future steps would include rescuing the candidate plasmids from CHP2489 and sequencing them. The candidates will be sequenced in order to detect altered amino acid residues. Some crystal structures of AC catalytic domains exist that would allow one to locate and characterize a potential binding site of the BCAC compound. Biochemical manipulation of the binding site could then possibly occur in the context of drug refinement.

Optimization of the genetic screen should be considered through repetition and through examining different cell densities at which cultures are inoculated with compounds, as preliminary experiments have suggested that the control strain shows the greatest shift in GFP signal after compound treatment when it is at a cell density of 10^6 cells/mL. Detection of a compound-resistant mutant allele is an imposing ambition, and the work that led to the design of the molecular genetic screen as outlined can serve as a foundation for analysis of other compound-sensitive AC alleles.

LITERATURE CITED

Bailey C. R., C. J. Bruton, M. J. Butler, K. F. Chater, J. E. Harris, *et al.*, 1986 Properties of in vitro recombinant derivatives of pJV1, a multi-copy plasmid from Streptomyces phaeochromogenes. J Gen Microbiol 132: 2071–2078. https://doi.org/10.1099/00221287-132-8-2071

Bender A. T., and J. A. Beavo, 2006 Cyclic nucleotide phosphodiesterases: molecular regulation to clinical use. Pharmacol Rev 58: 488–520. https://doi.org/10.1124/pr.58.3.5

Biel M., and S. Michalakis, 2009 Cyclic Nucleotide-Gated Channels, pp. 111–136 in *cGMP: Generators, Effectors and Therapeutic Implications*, Handbook of Experimental Pharmacology. edited by Schmidt H. H. H. W., Hofmann F., Stasch J.-P. Springer, Berlin, Heidelberg.

Burgin A. B., O. T. Magnusson, J. Singh, P. Witte, B. L. Staker, *et al.*, 2010 Design of phosphodiesterase 4D (PDE4D) allosteric modulators for enhancing cognition with improved safety. Nat Biotechnol 28: 63–70. https://doi.org/10.1038/nbt.1598

Chang G.-W., C.-C. Hsiao, Y.-M. Peng, F. A. Vieira Braga, N. A. M. Kragten, *et al.*, 2016 The Adhesion G Protein-Coupled Receptor GPR56/ADGRG1 Is an Inhibitory Receptor on Human NK Cells. Cell Reports 15: 1757–1770. https://doi.org/10.1016/j.celrep.2016.04.053

Dessauer C. W., V. J. Watts, R. S. Ostrom, M. Conti, S. Dove, *et al.*, 2017 International Union of Basic and Clinical Pharmacology. CI. Structures and Small Molecule Modulators of Mammalian Adenylyl Cyclases. Pharmacol Rev 69: 93–139. https://doi.org/10.1124/pr.116.013078

Domin M., and C. S. Hoffman, 2022 Methods to Assess Phosphodiesterase and/or Adenylyl Cyclase Activity Via Heterologous Expression in Fission Yeast, pp. 93–104 in *cAMP Signaling: Methods and Protocols*, Methods in Molecular Biology. edited by Zaccolo M. Springer US, New York, NY.

Eberhard J., and C. S. Hoffman, cAMP export by the fission yeast Schizosaccharomyces pombe. MicroPubl Biol 2021: 10.17912/micropub.biology.000384. https://doi.org/10.17912/micropub.biology.000384

Getz R. A., G. Kwak, S. Cornell, S. Mbugua, J. Eberhard, *et al.*, 2019 A fission yeast platform for heterologous expression of mammalian adenylyl cyclases and high throughput screening. Cellular Signalling 60: 114–121. https://doi.org/10.1016/j.cellsig.2019.04.010

Gutz H., Heslot H., Leupold U., Loprieno N., 1974 Schizosaccharomyces pombe, pp. 395–446 in *Handbook of Genetics*, edited by King R. C. Plenum Press, New York.

Hoffman C. S., and F. Winston, 1987 A ten-minute DNA preparation from yeast efficiently releases autonomous plasmids for transformation of Escherichia coli. Gene 57: 267–272. https://doi.org/10.1016/0378-1119(87)90131-4

Hoffman C. S., and F. Winston, 1989 A transcriptionally regulated expression vector for the fission yeast Schizosaccharomyces pombe. Gene 84: 473–479. https://doi.org/10.1016/0378-1119(89)90523-4

Hoffman C. S., and F. Winston, 1990 Isolation and characterization of mutants constitutive for expression of the fbp1 gene of Schizosaccharomyces pombe. Genetics 124: 807–816. https://doi.org/10.1093/genetics/124.4.807

Hoffman C. S., 2005a Glucose sensing via the protein kinase A pathway in Schizosaccharomyces pombe. Biochemical Society Transactions 33: 257–260. https://doi.org/10.1042/BST0330257

Hoffman C. S., 2005b Except in Every Detail: Comparing and Contrasting G-Protein Signaling in *Saccharomyces cerevisiae* and *Schizosaccharomyces pombe*. Eukaryot Cell 4: 495–503. https://doi.org/10.1128/EC.4.3.495-503.2005

Hoffman C. S., and F. Winston, Glucose repression of transcription of the Schizosaccharomycespombe fbpl gene occurs by a cAMP signaling pathway. 12.

Husted A. S., M. Trauelsen, O. Rudenko, S. A. Hjorth, and T. W. Schwartz, 2017 GPCR-Mediated Signaling of Metabolites. Cell Metabolism 25: 777–796. https://doi.org/10.1016/j.cmet.2017.03.008

Devoti, J., Seydoux, G., Beach D., M. McLeod, 1991 Interaction between ran1+ protein kinase and cAMP dependent protein kinase as negative regulators of fission yeast meiosis. EMBO Journal 10: 3759–3768. https://doi.org/10.1002/j.1460-2075.1991.tb04945.x

Ivey F. D., L. Wang, D. Demirbas, C. Allain, and C. S. Hoffman, 2008 Development of a fission yeast-based high-throughput screen to identify chemical regulators of cAMP phosphodiesterases. J Biomol Screen 13: 62–71. https://doi.org/10.1177/1087057107312127

Kamenetsky M., S. Middelhaufe, E. M. Bank, L. R. Levin, J. Buck, *et al.*, 2006 Molecular details of cAMP generation in mammalian cells: a tale of two systems. J Mol Biol 362: 623–639. https://doi.org/10.1016/j.jmb.2006.07.045

Kaur J., M. Soto-Velasquez, Z. Ding, A. Ghanbarpour, M. A. Lill, *et al.*, 2019 Optimization of a 1,3,4-oxadiazole series for inhibition of Ca2+/calmodulin-stimulated activity of adenylyl cyclases 1 and 8 for the treatment of chronic pain. European Journal of Medicinal Chemistry 162: 568–585. https://doi.org/10.1016/j.ejmech.2018.11.036

Kelly D. A., and C. S. Hoffman, 2002 Gap repair transformation in fission yeast to exchange plasmid-selectable markers. Biotechniques 33: 978, 980, 982. https://doi.org/10.2144/02335bm02

Lambright D. G., J. Sondek, A. Bohm, N. P. Skiba, H. E. Hamm, *et al.*, 1996 The 2.0 Å crystal structure of a heterotrimeric G protein. Nature 379: 311–319. https://doi.org/10.1038/379311a0

Levin L. R., and J. Buck, 2015 Physiological Roles of Acid-Base Sensors. Annual Review of Physiology 77: 347–362. https://doi.org/10.1146/annurev-physiol-021014-071821

Levine M. A., 1999 Clinical implications of genetic defects in G proteins: oncogenic mutations in G alpha s as the molecular basis for the McCune-Albright syndrome. Arch Med Res 30: 522–531. https://doi.org/10.1016/s0188-4409(99)00075-2

Maurice D. H., H. Ke, F. Ahmad, Y. Wang, J. Chung, *et al.*, 2014 Advances in targeting cyclic nucleotide phosphodiesterases. Nat Rev Drug Discov 13: 290–314. https://doi.org/10.1038/nrd4228

Medeiros A. S. de, A. Magee, K. Nelson, L. Friedberg, K. Trocka, *et al.*, 2013 Use of PKA-mediated phenotypes for genetic and small-molecule screens in Schizosaccharomyces pombe. Biochemical Society Transactions 41: 1692–1695. https://doi.org/10.1042/BST20130159

Muteeb G., and R. Sen, 2010 Random Mutagenesis Using a Mutator Strain, pp. 411–419 in *In Vitro Mutagenesis Protocols: Third Edition*, Methods in Molecular Biology. edited by Braman J. Humana Press, Totowa, NJ.

Neely L. A., and C. S. Hoffman, 2000 Protein Kinase A and Mitogen-Activated Protein Kinase Pathways Antagonistically Regulate Fission Yeast fbp1Transcription by Employing Different Modes of Action at Two Upstream Activation Sites. Molecular and Cellular Biology 20: 6426–6434. https://doi.org/10.1128/MCB.20.17.6426-6434.2000

Pavlos N. J., and P. A. Friedman, 2017 GPCR Signaling and Trafficking: The Long and Short of It. Trends in Endocrinology & Metabolism 28: 213–226. https://doi.org/10.1016/j.tem.2016.10.007

Rodbell M., 1995 Signal transduction: evolution of an idea. Environmental Health Perspectives 103: 8.

Roth M. Y., and J. K. Amory, 2016 Beyond the Condom: Frontiers in Male Contraception. Semin Reprod Med 34: 183–190. https://doi.org/10.1055/s-0036-1571435

Seifert R., G. H. Lushington, T.-C. Mou, A. Gille, and S. R. Sprang, 2012 Inhibitors of membranous adenylyl cyclases. Trends Pharmacol Sci 33: 64–78. https://doi.org/10.1016/j.tips.2011.10.006

Simonds W. F., 1999 G protein regulation of adenylate cyclase. Trends in Pharmacological Sciences 20: 66–73. https://doi.org/10.1016/S0165-6147(99)01307-3

Steegborn C., 2014 Structure, mechanism, and regulation of soluble adenylyl cyclases - similarities and differences to transmembrane adenylyl cyclases. Biochim Biophys Acta 1842: 2535–2547. https://doi.org/10.1016/j.bbadis.2014.08.012

Stiefel J., L. Wang, D. A. Kelly, R. T. K. Janoo, J. Seitz, *et al.*, 2004 Suppressors of an Adenylate Cyclase Deletion in the Fission Yeast Schizosaccharomyces pombe. Eukaryotic Cell 3: 610–619. https://doi.org/10.1128/EC.3.3.610-619.2004

Sutherland E. W., G. A. Robison, and R. W. Butcher, 1968 Some Aspects of the Biological Role of Adenosine 3',5'-monophosphate (Cyclic AMP). Circulation 37: 279–306. https://doi.org/10.1161/01.CIR.37.2.279

Vassarotti A., and J. D. Friesen, 1985 Isolation of the fructose-1,6-bisphosphatase gene of the yeast Schizosaccharomyces pombe. Evidence for transcriptional regulation. J Biol Chem 260: 6348–6353.

Weinstein L. S., M. Chen, T. Xie, and J. Liu, 2006 Genetic diseases associated with heterotrimeric G proteins. Trends in Pharmacological Sciences 27: 260–266. https://doi.org/10.1016/j.tips.2006.03.005

Yamamoto T., V. C. Manganiello, and M. Vaughan, 1983 Purification and characterization of cyclic GMP-stimulated cyclic nucleotide phosphodiesterase from calf liver. Effects of divalent cations

on activity. Journal of Biological Chemistry 258: 12526–12533. https://doi.org/10.1016/S0021-9258(17)44208-6

Yamamoto M., 1996 The molecular control mechanisms of meiosis in fission yeast. Trends in Biochemical Sciences 21: 18–22. https://doi.org/10.1016/S0968-0004(06)80022-8

Zhang G., Y. Liu, A. E. Ruoho, and J. H. Hurley, 1997 Structure of the adenylyl cyclase catalytic core. Nature 386: 247–253. https://doi.org/10.1038/386247a0